

2

DTIC FILE COPY

# NAVAL POSTGRADUATE SCHOOL Monterey, California

AD-A218 706



DTIC  
ELECTE  
FEB 15 1990  
S B D  
Co

## THESIS

THE LITHIUM CONCENTRATION DEPENDENCE OF  
CREEP IN BINARY ALUMINUM-LITHIUM ALLOYS

by

David Wayne Taylor

June 1989

Thesis Advisor: Terry R. McNelley

Approved for public release; distribution is unlimited.

Unclassified

Security Classification of this page

REPORT DOCUMENTATION PAGE

1a Report Security Classification <b>Unclassified</b>		1b Restrictive Markings	
2a Security Classification Authority		3 Distribution Availability of Report	
2b Declassification/Downgrading Schedule		Approved for public release; distribution is unlimited	
4 Performing Organization Report Number(s)		5 Monitoring Organization Report Number(s)	
6a Name of Performing Organization	6b Office Symbol <i>(If Applicable)</i> 69	7a Name of Monitoring Organization	
Naval Postgraduate School		Naval Postgraduate School	
6c Address (city, state, and ZIP code)		7b Address (city, state, and ZIP code)	
Monterey, CA 93943-5000		Monterey, CA 93943-5000	
8a Name of Funding/Sponsoring Organization	8b Office Symbol <i>(If Applicable)</i>	9 Procurement Instrument Identification Number	
8c Address (city, state, and ZIP code)		10 Source of Funding Numbers	
		Program Element Number	Project No
		Task No	Work Unit Accession No

11 Title (include Security Classification) **Lithium Concentration Dependence of Creep in Binary Aluminum-Lithium Alloys**

12 Personal Author(s) **David Wayne Taylor**

13a Type of Report	13b Time Covered	14 Date of Report (year, month, day)	15 Page Count
Master's Thesis	From	June 1989	56

16 Supplementary Notation The views expressed in this thesis are those of the author and do not reflect the official policy or position of the Department of Defense or the U.S. Government.

17 Cosan Codes			18 Subject Terms (continue on reverse if necessary and identify by block number)
Field	Group	Subgroup	

Creep, Aluminum-Lithium Alloys, Thermomechanical Processing, Temperature Dependence, Stress Dependence, Subgrains

19 Abstract (continue on reverse if necessary and identify by block number)

An investigation was conducted into the concentration dependence of creep of binary Al-Li alloys. Constant true-stress creep and constant extension-rate stress-strain tests were conducted at temperatures ranging from 250°C to 500°C. Optical microscopy demonstrated that subgrains formed during deformation and that the predominant physical processes in the creep of Al-Li alloys appears to be dislocation climb, with Lithium providing strengthening by its effect on the modulus or the stacking fault energy.

20 Distribution Availability of Abstract		21 Abstract Security Classification	
<input checked="" type="checkbox"/> unclassified/unlimited	<input type="checkbox"/> same as report	<input type="checkbox"/> DTIC users	<b>Unclassified</b>
22a Name of Responsible Individual		22b Telephone (include Area code)	22c Office Symbol
Professor T. R. McNelley		(408) 646-3589	69Mc

Approved for public release; distribution is unlimited.

**The Lithium Concentration Dependence of Creep  
In Binary Aluminum-Lithium Alloys**

by

David Wayne Taylor  
Lieutenant Commander, United States Navy  
B.S.E.E., University of Washington, 1975

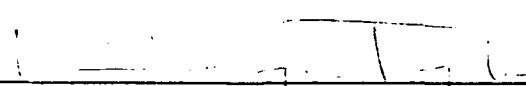
Submitted in partial fulfillment of the  
requirements for the degree of

MASTER OF SCIENCE IN MECHANICAL ENGINEERING

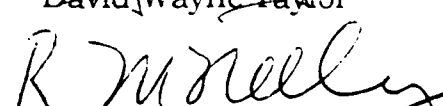
from the

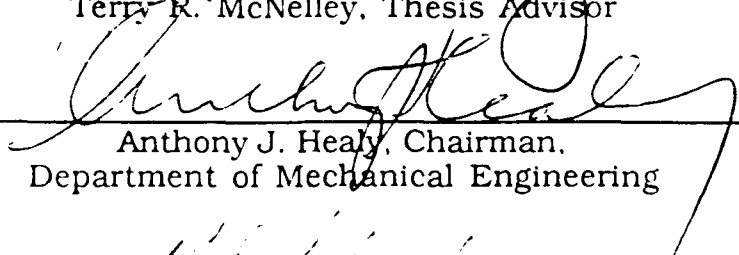
NAVAL POSTGRADUATE SCHOOL  
June 1989

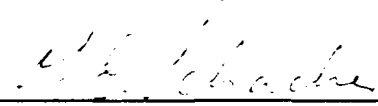
Author:

  
\_\_\_\_\_  
David Wayne Taylor

Approved by:

  
\_\_\_\_\_  
Terry R. McNelley, Thesis Advisor

  
\_\_\_\_\_  
Anthony J. Healy, Chairman,  
Department of Mechanical Engineering

  
\_\_\_\_\_  
Gordon E. Schacher, Dean of  
Science and Engineering

## ABSTRACT

An investigation was conducted into the concentration dependence of creep of binary Al-Li alloys. Constant true-stress creep and constant extension-rate stress-strain tests were conducted at temperatures ranging from 250° C to 500° C. Optical microscopy demonstrated that subgrains formed during deformation and that the predominant physical processes in the creep of Al-Li alloys appears to be dislocation climb, with Lithium providing strengthening by its effect on the modulus or the stacking fault energy.

For	
SI	<input checked="" type="checkbox"/>
ed	<input type="checkbox"/>
tion	<input type="checkbox"/>

Distribution/	
Library Codes	
Dist	Special
A-1	

## TABLE OF CONTENTS

<b>I. INTRODUCTION.....</b>	<b>1</b>
<b>II. BACKGROUND .....</b>	<b>3</b>
A. SCOPE OF RESEARCH .....	3
B. THE STRUCTURE OF AL-LI ALLOYS.....	4
C. CREEP OF PURE METALS .....	5
D. CREEP MECHANISMS.....	5
E. STRESS DEPENDENCE AND ACTIVATION ENERGY.....	6
<b>III. EXPERIMENTAL PROCEDURE.....</b>	<b>9</b>
A. SAMPLE PROCESSING AND FABRICATION.....	9
B. TESTING.....	10
1. Self-Aligning Grips .....	11
2. Instron Testing.....	11
3. Creep Testing.....	13
C. MICROSCOPY.....	16
<b>IV. RESULTS AND DISCUSSION.....</b>	<b>17</b>
A. MICROSCOPY.....	17
B. MECHANICAL RESPONSE.....	17
C. STRAIN RATE DEPENDENCE OF STRESS.....	22

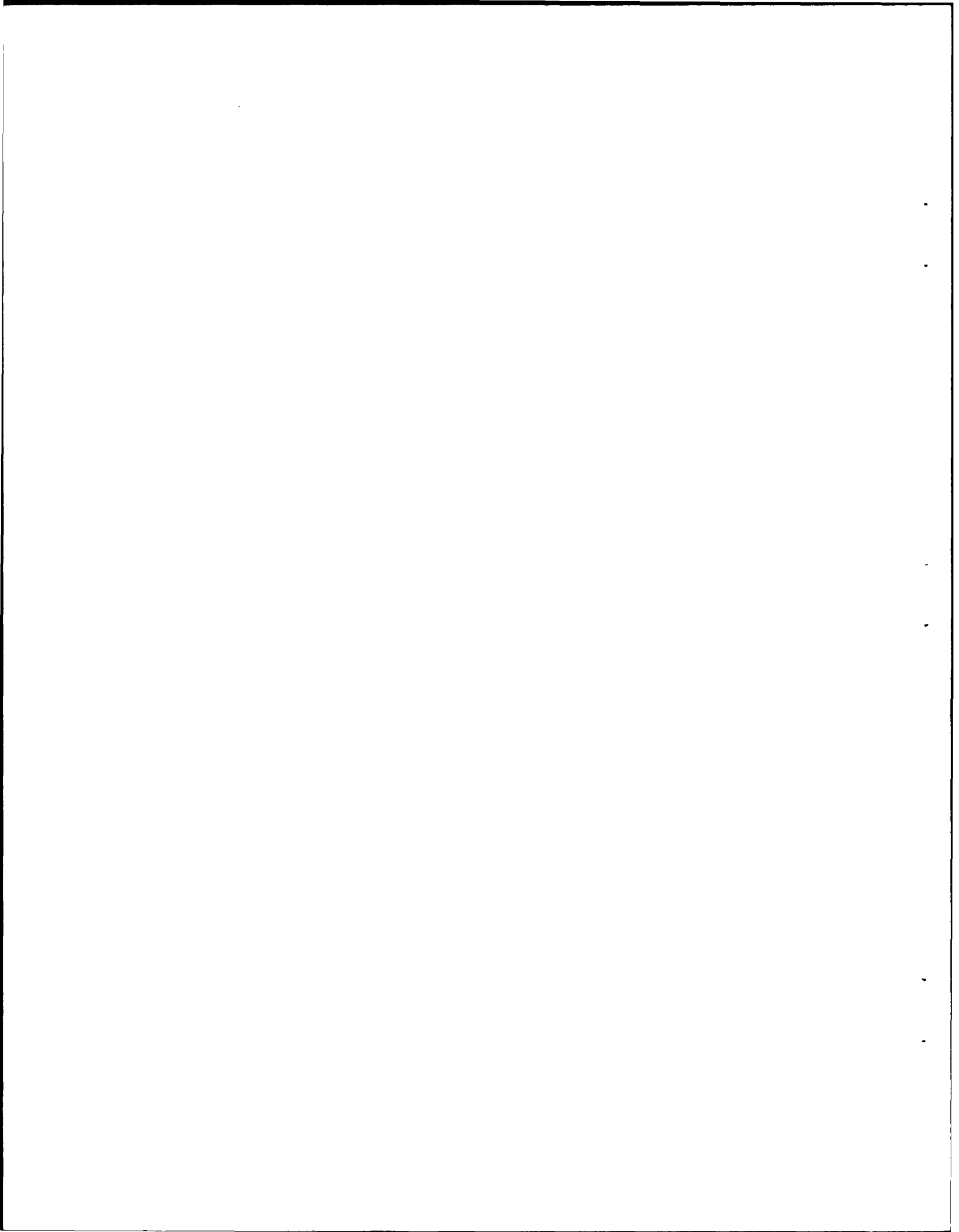
D. EFFECT OF DEFORMATION ON MICROSTRUCTURE.....	30
E. ACTIVATION ENERGY.....	35
F. EFFECT OF LITHIUM CONCENTRATION ON STRENGTH....	37
G. NORMALIZED RESULTS.....	41
<b>V. CONCLUSIONS.....</b>	<b>44</b>
LIST OF REFERENCES.....	46
BIBLIOGRAPHY.....	48
INITIAL DISTRIBUTION LIST.....	50

## LIST OF FIGURES

1.	Aluminum-Lithium Phase Diagram.....	3
2.	Creep Sample Geometry .....	10
3.	Self-Centering Grip Assembly.....	12
4.	Constant Stress Creep Apparatus .....	14
5.	As Rolled 1.0% Lithium.....	18
6.	Annealed, Unstrained 1.0% Lithium.....	18
7.	Effect of Strain Rate (Instron).....	19
8.	Effect of Lithium Concentration (Instron).....	20
9.	Effect of Temperature (Instron).....	21
10.	Creep Results for 0.5% Li at 400° C $\sigma = 6.61 \text{ MPA}$ , $\dot{\epsilon} = 1.74 \times 10^{-4} \text{ sec}^{-1}$ .....	23
11.	Creep Results for 0.5% Li at 400° C $\sigma = 4.13 \text{ MPA}$ , $\dot{\epsilon} = 2.58 \times 10^{-5} \text{ sec}^{-1}$ .....	24
12.	Creep Results for 1.0% Li at 500° C $\sigma = 2.5 \text{ MPA}$ , $\dot{\epsilon} = 1.29 \times 10^{-4} \text{ sec}^{-1}$ .....	25
13.	Log $\dot{\epsilon}$ vs. Log $\sigma$ Results (0.5% Li) .....	31
14.	Log $\dot{\epsilon}$ vs. Log $\sigma$ Results (1.0% Li) .....	32
15.	0.5% Li at 400° C, $\dot{\epsilon} = 1.67 \times 10^{-2} \text{ sec}^{-1}$ .....	33
16.	0.5% Li at 500° C, $\dot{\epsilon} = 1.67 \times 10^{-2} \text{ sec}^{-1}$ .....	33
17.	1.0% Li at 400° C, $\dot{\epsilon} = 1.67 \times 10^{-2} \text{ sec}^{-1}$ .....	34
18.	1.0% Li at 500° C, $\dot{\epsilon} = 1.67 \times 10^{-2} \text{ sec}^{-1}$ .....	35
19.	$\dot{\epsilon}$ vs. $\sigma$ at 250° C .....	38
20.	$\dot{\epsilon}$ vs. $\sigma$ at 350° C .....	39

21.	$\dot{\epsilon}$ vs. $\sigma$ at 500° C .....	40
22.	Normalized Results 0.5% Li.....	42
23.	Normalized Results 1.0% Li.....	43





## I. INTRODUCTION

Because of good ductility and forming characteristics, excellent corrosion resistance, and a potential for a high strength-to-weight ratio, Aluminum alloys have been used in a wide variety of structural applications, most notably for fabrication of aerospace vehicles. To attempt to better compete with emerging technologies such as composite materials and to give designers a broader range of choices, metallurgists have attempted to improve upon the physical properties of Aluminum alloys by various means, including consideration of new alloying elements.

One such candidate for addition is Lithium. At ambient temperatures, one weight percent Lithium added to Aluminum (up to four weight percent) reduces the alloy density by three percent and increases the elastic modulus by six percent [Ref. 1]. To date, essentially all research concerned with the strength and ductility of Aluminum-Lithium alloys has been conducted at or below ambient temperatures.

External surfaces on high-speed aircraft are subjected to elevated temperatures due to aerothermic heating. The wing surfaces of the Concorde supersonic aircraft may reach temperatures as high as 100° C in flight. There is, however, virtually no information contained in the literature describing the physical and mechanical behavior of Aluminum-Lithium alloys at elevated temperatures.

The purpose of this research is to examine the mechanical behavior of binary Aluminum-Lithium alloys at elevated temperatures. This includes an examination of the Lithium contribution to strength at elevated temperatures (from 250° C to 500° C) and the effect of Lithium concentration on creep deformation mechanisms. At such temperatures, Li will be in solid solution. Subsequent research should examine creep at lower temperatures where precipitate structures will also be present.

## II. BACKGROUND

### A. SCOPE OF RESEARCH

This research considered Lithium concentrations of 0.5 and 1.0 weight percent and test temperatures from 250° to 500° C. In this temperature range, both alloys will remain well within the solid solution region on the phase diagram (Figure 1) [Refs. 2, 3].

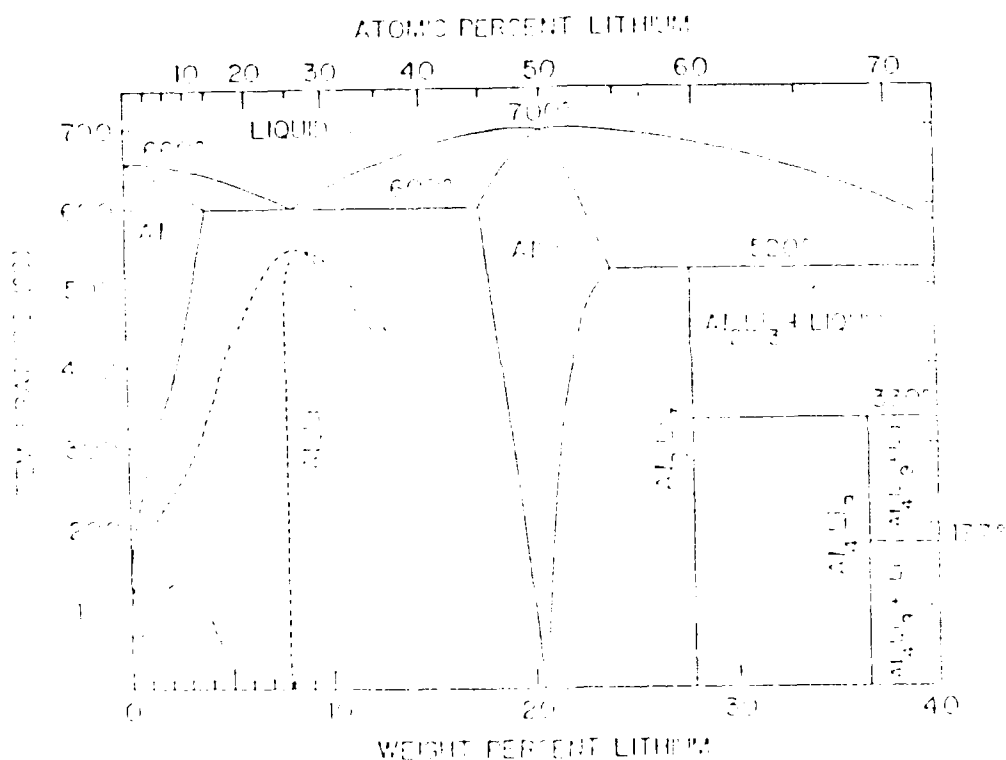


Figure 1. Aluminum-Lithium Phase Diagram

By restricting testing to this region, the effects of solid solution strengthening alone can be examined, uncomplicated by any influence of precipitation strengthening.

## **B. THE STRUCTURE OF AL-LI ALLOYS**

The increased modulus of elasticity resulting from the addition of Lithium to Aluminum has been addressed by Fox [Ref. 4] in a study of alloys containing 1.33 and 2.14 weight percent Li. He reported that the addition of Lithium results in an increase in the electron charge density because the nearest neighbor (N.N.) distance in these alloys is about six percent less than the distance in pure Lithium. Because of this decreased distance, the force constant between Lithium atoms is increased. Rudmilovic and Fox [Ref. 5] also reported that these same alloys exhibit evidence for ordering within the solid solution range of the phase diagram. This conclusion was based on the presence in brine-quenched samples of superlattice reflections and no discernable second-phase precipitate particles. In fact, the existence of such an ordered structure would facilitate decomposition of the solid solution by a spinodal reaction and explain the difficulty in suppressing precipitation in alloys containing more than 1.6 weight percent Li.

The increased modulus and existence of ordering in the solid solution both reflect a tendency of Al and Li to bond. The temperature dependence of the Al-Li interaction has not been addressed. The modulus of elasticity, as well as other material factors such as stacking fault energy, are known to influence creep of metals and alloys [Ref. 3]. Thus, it may be anticipated that the creep response of Al-Li alloys may reflect these factors.

### C. CREEP OF PURE METALS

For pure metals deformed under creep conditions, the true creep strain plotted as a function of time exhibits three distinct stages. The first stage is a period of decreasing creep rate as the metal hardens. Substructures formed during this stage are strongly dependent on creep stress.

The next stage, secondary creep, is an interval of a constant creep rate. During this stage, substructures generally are unchanged.

Tertiary creep is generally associated with a rapid increase in creep rate, with necking and eventual failure.

### D. CREEP MECHANISMS

Sherby and Burke [Ref. 6] state that creep response in solid solution alloys in the intermediate range in  $\frac{\dot{\epsilon}}{D}$  values from  $10^2 \text{ cm}^{-2}$  to  $10^9 \text{ cm}^{-2}$  (where  $\dot{\epsilon}$  is the strain rate normalized for temperature by the diffusion coefficient  $D$ ) can be placed in two categories. The first, denoted Class I, follow a constitutive law of the form:

$$\dot{\epsilon} = BD_s \left( \frac{\sigma}{E} \right)^3 \quad (1)$$

where  $\dot{\epsilon}$  is the strain rate,  $D_s$  is the diffusion coefficient of the solute,  $\sigma$  is the stress,  $E$  is the modulus of elasticity, and  $B$  is a constant. The mechanism of creep for these alloys is controlled by the process of dislocation glide, the rate of which is determined by the velocity at which solute atoms can be dragged along with moving dislocations. Creep in this class of alloys appears to be unaffected by such factors as

subgrain size or stacking fault energy and does not exhibit significant primary creep. The factors that do appear to affect creep in these alloys are the diffusion coefficient of the solute and the modulus of the solid solution.

Conversely, Class II alloys follow a constitutive law of the form:

$$\dot{\epsilon} = AD_l \gamma^3 \left( \frac{\sigma}{E} \right)^5 \quad (2)$$

where  $\gamma$  is the stacking fault energy,  $D_l$  is the lattice diffusion coefficient,  $E$  is the elastic modulus, and  $A$  is a physical constant. The mechanism of creep in this class is dislocation climb, the rate of which is affected by subgrain size, stacking fault energy, and modulus, as are the creep rates of pure metals. Also, Class II alloys exhibit a distinct primary creep phase.

Stacking fault energy and modulus are temperature dependent, and this dependence is well documented for pure Aluminum. However, there exists virtually no data concerning the temperature dependence for modulus and stacking fault energy for solid solution Aluminum-Lithium alloys.

#### **E. STRESS DEPENDENCE AND ACTIVATION ENERGY**

The stress dependence of the creep rate may be evaluated experimentally by the determination of the stress exponent  $n = d \ln \dot{\epsilon} / d \ln \sigma$  for test data. Similarly, diffusion coefficients are of the form

$$D = D_0 \exp\left(-\frac{Q}{RT}\right) \quad (3)$$

where  $D_0$  is a constant,  $Q$  is the activation energy,  $R$  is the gas constant, and  $T$  is the temperature. Thus, the temperature dependence of deformation may be expected to be of the form

$$Q_c = -R \frac{\partial \ln \dot{\epsilon}}{\partial \left(\frac{1}{T}\right)} \quad (4)$$

where  $Q_c$  is the activation energy which will be equal to that for either solute diffusion,  $Q_s$ , or lattice diffusion,  $Q_D$ , depending upon the deformation mechanism.

If the assumption is made that the Aluminum-Lithium alloys exhibit Class I behavior, one would expect that they would show a stress exponent  $n = 3$ . Additionally, the activation energy for deformation of the alloy would be equal to the activation energy for diffusion of the Lithium solute, and little evidence of subgrain formation would be noted in the course of metallographic investigations.

If, on the other hand, Al-Li alloys were to exhibit Class II behavior, then according to equation 2 the stress exponent  $n$  could be anticipated to be 5, with the activation energy for deformation the same as the activation energy for self-diffusion.

However, if the temperature dependence of the stacking fault energy  $\gamma$  or the modulus  $E$  is sufficient, such dependence may affect the observed value of activation energy. Activation energy for creep of Class II at a constant stress can then be expressed [Ref. 6] as:



$$Q_c = -R \frac{\partial \ln D}{\partial (\frac{1}{T})} + 5R \frac{\partial \ln E}{\partial (\frac{1}{T})} - 3R \frac{\partial \ln \gamma}{\partial (\frac{1}{T})} \quad (5)$$

$$= Q_D + 5R \frac{\partial \ln E}{\partial (\frac{1}{T})} - 3R \frac{\partial \ln \gamma}{\partial (\frac{1}{T})} \quad (6)$$

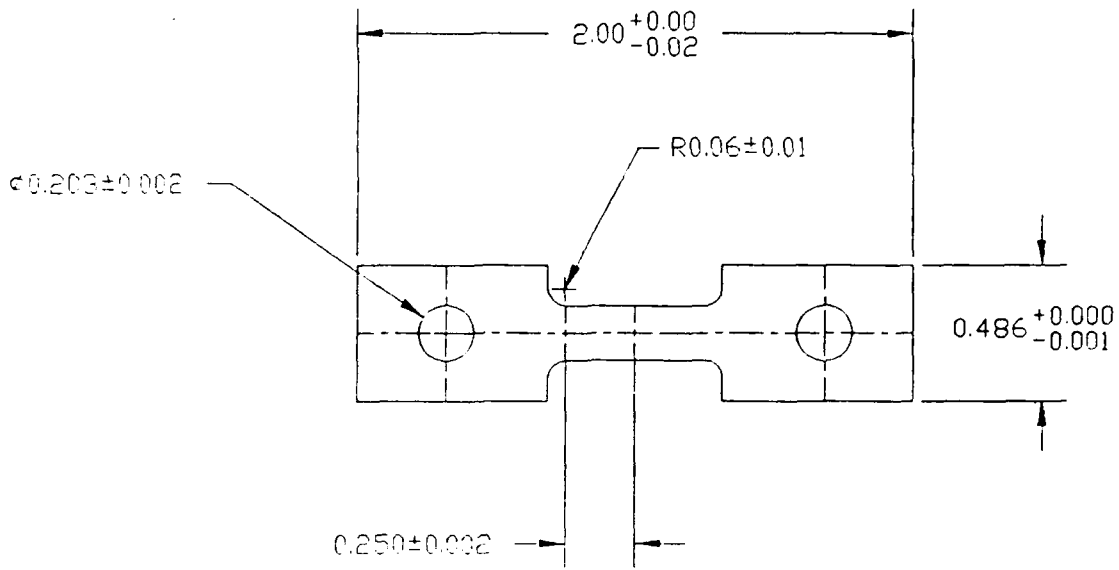
The first term is simply the activation energy for self-diffusion. If the stacking fault energy or modulus do not change appreciably with temperature, then equation 6 suggests the activation energy for creep will effectively be equal to the activation energy for self-diffusion, as noted. However, if  $\gamma$  and  $E$  are strongly temperature dependent, then activation energy for creep will differ substantially from the activation energy for self-diffusion.

### III. EXPERIMENTAL PROCEDURE

#### A. SAMPLE PROCESSING AND FABRICATION

The alloys studied in this research were cast at the Naval Surface Weapons Center (NSWC) in White Oak, Maryland, utilizing 99.99 percent pure Aluminum alloyed with 99.9 percent pure Lithium. The alloys were of nominal compositions Al -0.5 weight percent Li and Al -1.0 weight percent Li. The material received at the Naval Postgraduate School from NSWC was in the form of tapered cylindrical ingots 200 mm (8.0 in.) in length and approximately 76 mm (3.0 in.) in diameter. Transverse sections 42 mm (1.5 in.) thick were homogenized by annealing at 540° C for four hours and were hot rolled at temperatures between 400° C and 450° C to a final thickness of approximately 2.0 mm (.08 in.).

The rolled material was cut by band saw into rectangular specimen blanks and machined into reduced gauge section sheet-type "dogbone" tensile specimens with the long axis parallel to the rolling direction (see Figure 2). A special holding device was fabricated to secure the samples during machining due to the extreme softness and ductility of the material. Five specimens were machined at one time. The finished samples were examined for defects and all machining burrs were carefully removed with a jeweler's file. Prior to testing, all samples received a heat treatment of 15 minutes at 500° C, resulting in an equiaxed structure prior to testing.



(Dimensions are in inches)

Figure 2. Creep Sample Geometry

## B. TESTING

To obtain results from the widest range of stress and temperature for each concentration, two methods of testing were employed. The first method consisted of a series of constant extension-rate tests using an Instron machine. Samples were tested at strain rates from  $1.67 \times 10^{-2}/s^{-1}$  to  $1.67 \times 10^{-4}/s^{-1}$  (as dictated by available speeds on the machine) for the temperature range of  $250^{\circ}C$  to  $500^{\circ}C$  with  $50^{\circ}C$  intervals between test temperatures.

To achieve strain rates slower than the capability of the Instron machine, a constant true stress creep machine was employed. Applied loads were chosen to extend logically the range of tests performed on

the Instron. The temperature range and intervals employed were identical to those used for the Instron tests.

### **1. Self-Aligning Grips**

Special self-aligning grips for both tests were designed [Ref. 7] to hold the tensile test specimens. These grips (Figure 3) were fabricated of Inconel 625 alloy by Collins Instrument Company, Freeport, Texas, using a wire electro-discharge machining (EDM) process for tolerance control. Unique features of the grips include a tapered shank leading to a button head which aligns itself by transmitting load to the grips via the taper. The recessed face of the grips compressively hold the tab, applying load to the entire tab, not just the area above the bolt hole.

### **2. Instron Testing**

A model 1102 Instron machine with a 1,000-pound capacity load cell was used to conduct the faster strain rate tests. Extension rates chosen were a function of the available cross-head speeds of machine. For the sample gage length used, the strain rates of  $1.67 \times 10^{-2}$ ,  $1.67 \times 10^{-3}$ , and  $1.67 \times 10^{-4}$ , per second, corresponded to crosshead speeds of 0.5, 0.05, and 0.005 inches per minute. A Lindberg 59344 temperature controller in combination with a Marshall tubular furnace was used to heat the sample and grips, which in turn were suspended in a specially designed cage assembly. A temperature gradient of less than  $2^{\circ}\text{C}$  was established across the gauge length by installation of external shunt taps and temperatures were continuously

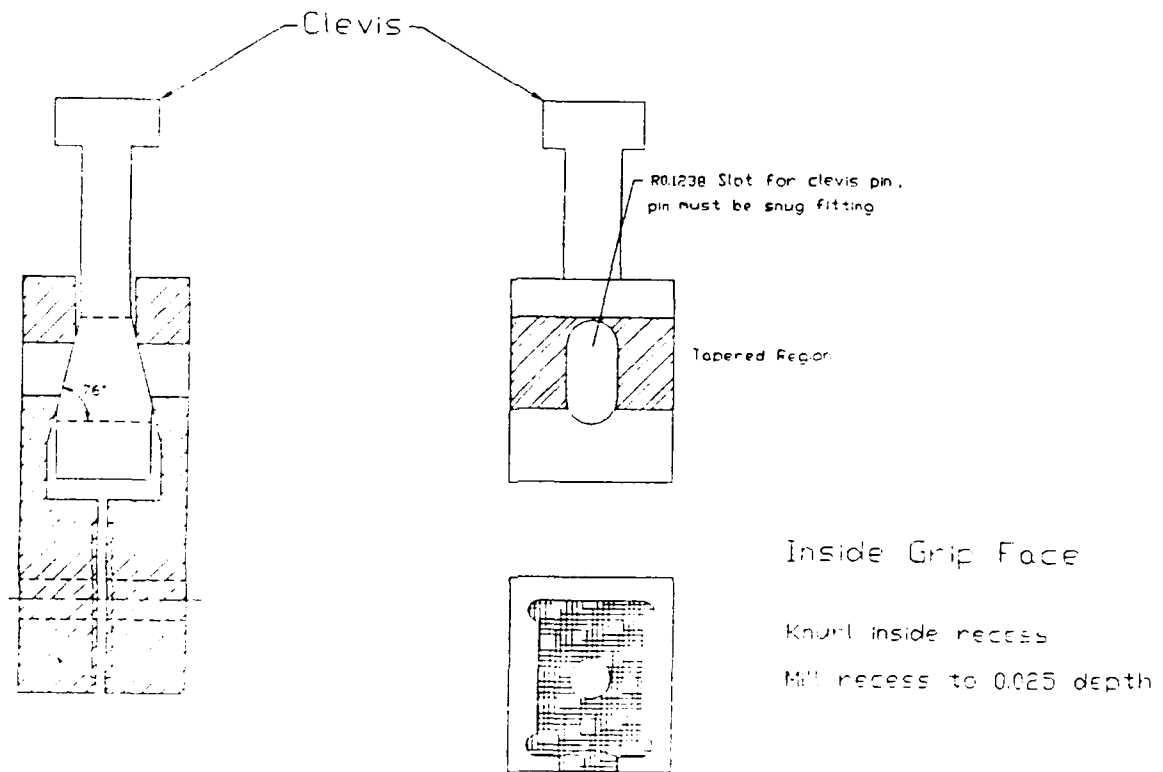


Figure 3. **Self-Centering Grip Assembly**

monitored throughout the duration of the testing via type "K" chromel-alumel thermocouples. Prior to testing, the furnace was raised, heated to test temperature, and held for 30 minutes. Once temperature was attained, the furnace was lowered and the grip assembly with sample installed was inserted into the grip holder assembly. The furnace was raised, re-energized, and allowed again to stabilize for approximately 20 minutes. Once at temperature, slack was removed from the load train and the test was initiated. As the entire gauge/grip/heater assembly is mounted to the bottom of the cross-head and moves down with the cross-head as the test progresses, the

original temperature gradient can be maintained for any extension likely to be encountered with these alloys.

Raw data, from the plastic region of deformation, was obtained manually from the Instron load vs. time strip chart output. These data were converted by a program written in Basic for an IBM PC to true stress vs. true strain in the plastic region. These data were plotted using an HP 7225B plotter.

The peak true stress from the above plot was paired with the known applied strain rate to determine a single data point. In general, this ultimate strength was observed over a range of strain suggesting deformation at a near-steady-state condition.

### **3. Creep Testing**

Creep testing was conducted on two creep machines using values of applied load to extend logically the previously determined Instron results. These machines (Figure 4), capable of transmitting loads between 1.5 and 222.5 Newtons (.3 to 50 lbs.) and at strains as high as 300 percent, were patterned after a machine built by Barrett, later modified by Matlock [Ref. 8]. The constant stress is obtained by means of an Andradre-Chalmers lever arm [Ref. 9]. The contoured lever rotates as the specimen is deformed. This rotation decreases the moment arm of the applied load as the cross-sectional area of the specimen decreases with elongation, thus maintaining a constant true stress. The design of the arm is based on the assumption that the load train is rigid and the linkage displacement is taken up uniformly.

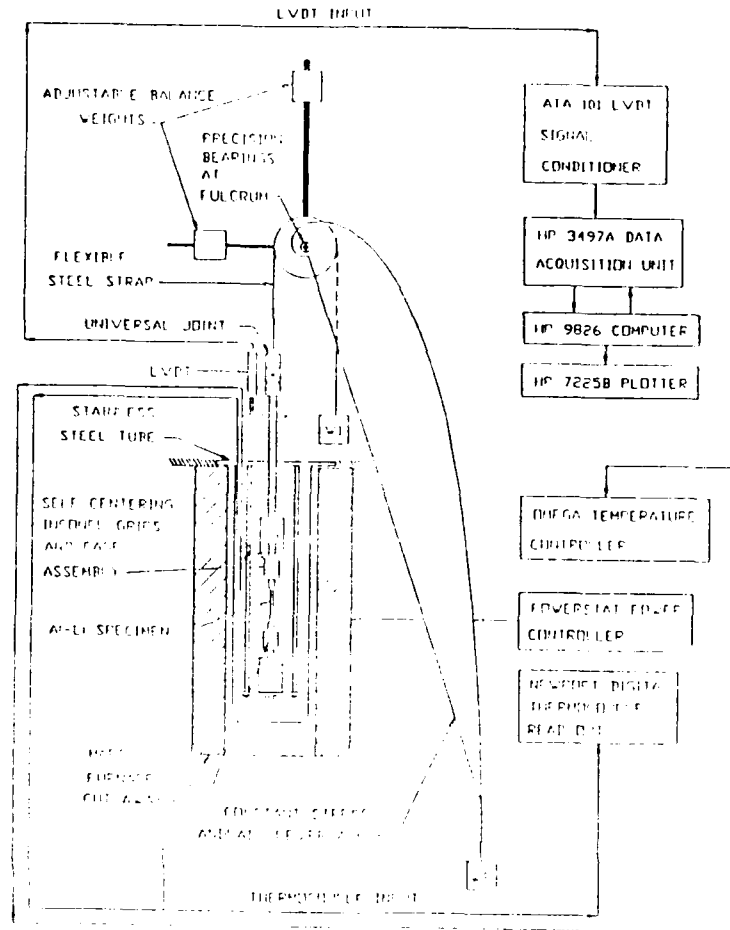


Figure 4. Constant Stress Creep Apparatus

The contour of the lever arm was designed using Autocad in conjunction with the highly accurate graphical technique developed by Coghlan [Ref. 10]. The design was based on an effective gauge length of 13 mm (0.5 in.) with an initial lever arm ratio of ten to one. The lever arm was constructed of 6.4 mm (.25 in.) thick 2024-T6 Aluminum and attached to a 9.53 mm (.375 in.) diameter shaft rotating on a set of precision bearings. An adjustable counterbalance was affixed to the opposite end of the shaft, balancing the lever arm. This counter-

balance, in conjunction with another attached to the shaft to compensate for the weight of the load train, insured that the only load sensed by the sample was that of the applied load.

A flexible .55 mm (.02 in.) thick steel strap follows the lever arm contour and hangs along the vertical tangent to the lever. A second flexible strap hangs tangent to a two-inch radius disc centered at the fulcrum point and transmits the tensile load to sample via the load train. The entire linkage was calibrated using a 50 lbf capacity interface load cell installed in the load train. The maximum stress variation experienced through 300 percent elongation was 1.4 percent.

Sample elongation was measured using a Schaevitz linear variable differential transformer (LVDT) with a one-inch displacement, with the core of the LVDT attached to the upper specimen linkage. The 2.866 mv/v signal from the LVDT is conditioned by a Schaevitz ATA 101 Analog Transducer Amplifier. The output was measured by an HP 3497A Data Acquisition Unit controlled by an HP9826 computer.

A 1200° C capacity Marshall tubular furnace was used to heat the creep sample and was powered by a 15 amp. Powerstat controlled by an Omega temperature controller. The temperature gradient was controlled and monitored in a similar manner to the Instron testing. Preheat and sample loading procedures were also similar.

When temperature was restabilized after loading the sample, the test program was initiated. The LVDT was zeroed (as determined with a digital multi-meter) in parallel with the ATA 101. A precalculated weight of lead shot (in a plastic bag) was carefully suspended



from the lever arm by the flexible strap at the lower end of the arm. Each test was allowed to continue to failure.

Data was stored to disc and plotted on the HP 7275B plotter. The creep rate in the secondary region was graphically determined from the true strain vs. time creep curve and was paired with the known applied stress to constitute a single data point.

### **C. MICROSCOPY**

Specimens were cut from as-rolled and annealed, untested samples as well as from specimens strained to failure at various temperatures. They were mounted in Buehler fast-cure acrylic, displaying the plan view of the tensile (and rolling) direction. Specimens were manually wet ground in successive steps of 220, 320, 400, and 600 grit using silicon carbide paper. The samples were then polished on diamond wheels with grit size 6, 3, and 1 micron, lubricated with Metadi solution. Final polishing, using Miromet Cerium Oxide polishing compound, prepared the samples for electro-etching. In this final step, the specimens were rinsed and electro-etched in Barker's reagent (25 ml  $\text{HBF}_4$  in 100 ml  $\text{H}_2\text{O}$ ) for 90 seconds at 20 volts. The specimens were immediately examined at 50x on a ICM 405 Zeiss microscope under polarized light. Significant microstructures were photographed using Kodak Panatomic-Y print film.

## IV. RESULTS AND DISCUSSION

### A. MICROSCOPY

Optical microscopy was conducted on as-rolled samples and on samples annealed at 500° C prior to stress-strain and creep testing. The as-rolled material (Figure 5) exhibited grains somewhat elongated in the rolling direction, consistent with the processes of fabrication. Subsequent annealing resulted in a microstructure that consisted of large, equiaxed grains (Figure 6). Thus, the anneal at 500° C for 15 minutes was sufficient to remove the effects of the rolling.

### B. MECHANICAL RESPONSE

Figure 7 summarizes typical results of Instron testing of the 0.5 percent Li alloy at 250° C and strain rates of  $1.67 \times 10^{-2}$ /second and  $1.67 \times 10^{-3}$ /second, respectively. Note that the material tested at the faster strain rate achieves a higher yield strength, rate of strain hardening, and maximum stress than that at the slower rate. For these conditions, strain hardening predominates the stress-strain curve and there is no apparent steady-state behavior.

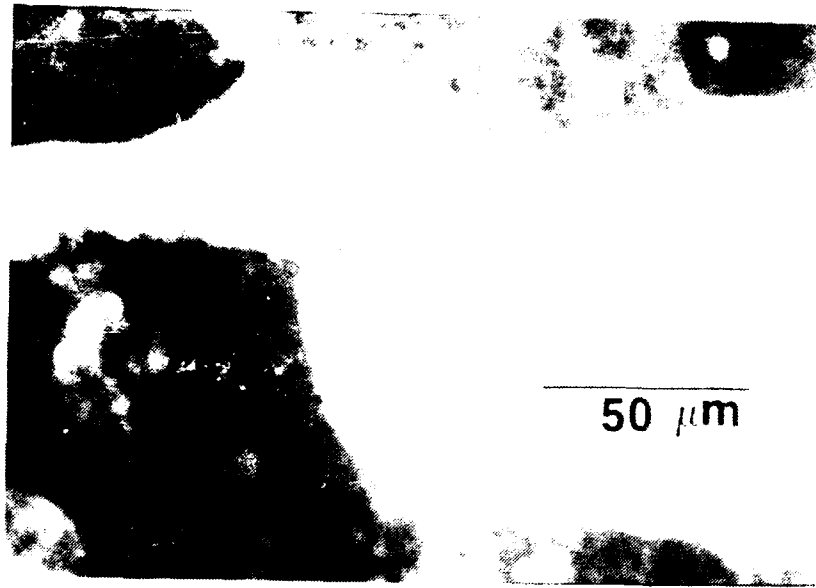


Figure 5. As Rolled 1.0% Lithium

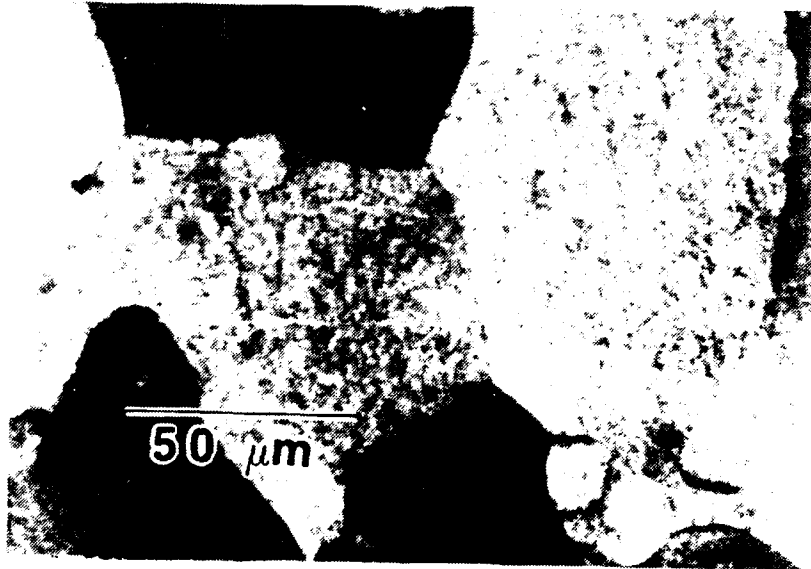
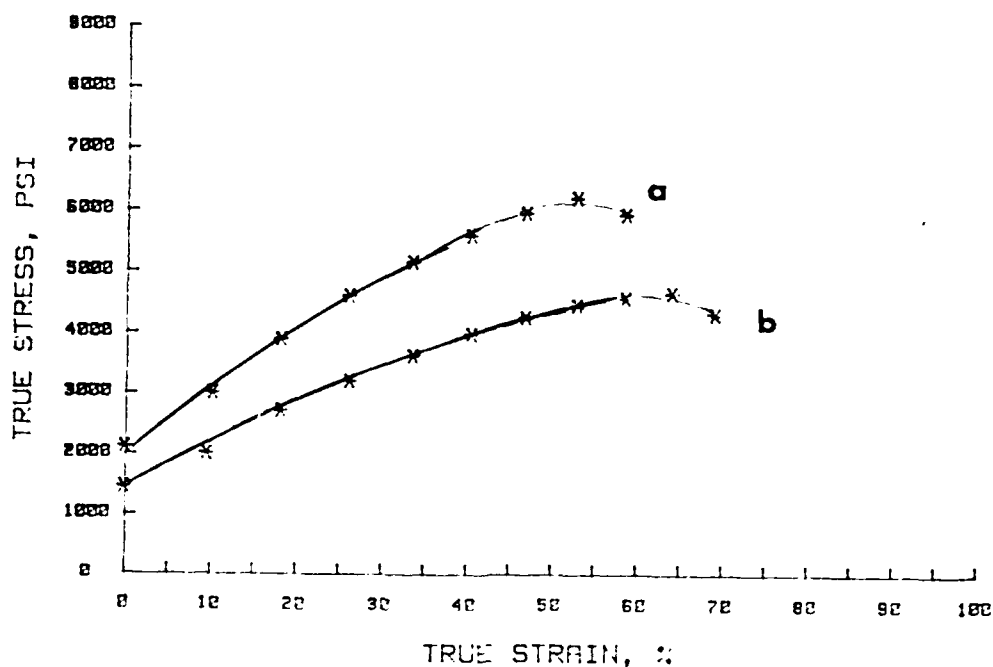


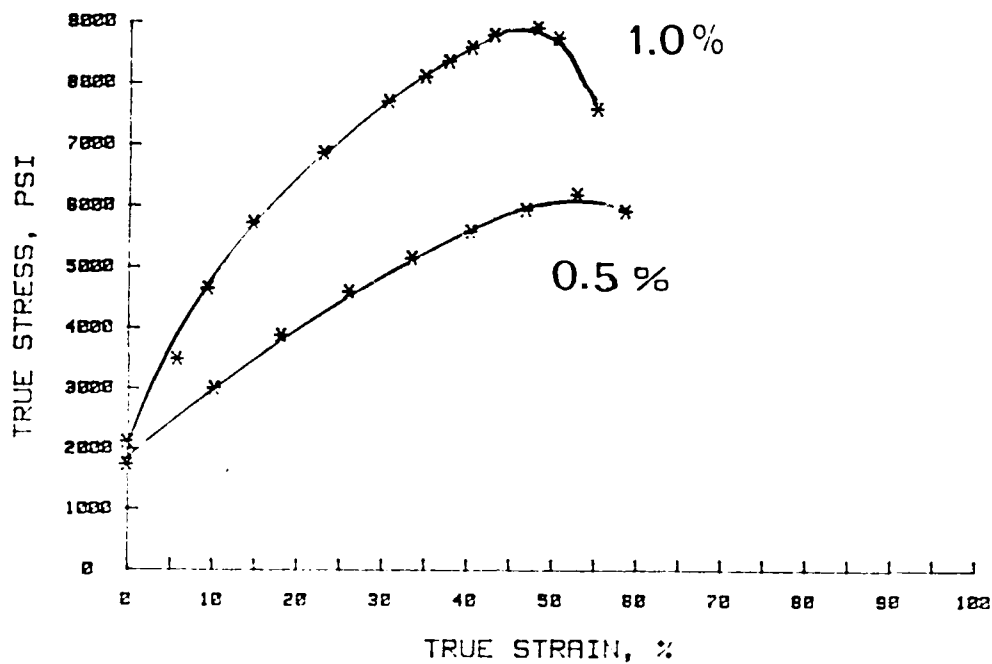
Figure 6. Annealed, Unstrained 1.0% Lithium



Samples of 0.5% Li tested at 250° C and  
 $\dot{\epsilon}$  = a)  $1.67 \times 10^{-2} \text{ sec}^{-1}$ ,  
 b)  $1.67 \times 10^{-3} \text{ sec}^{-1}$

Figure 7. Effect of Strain Rate (Instron)

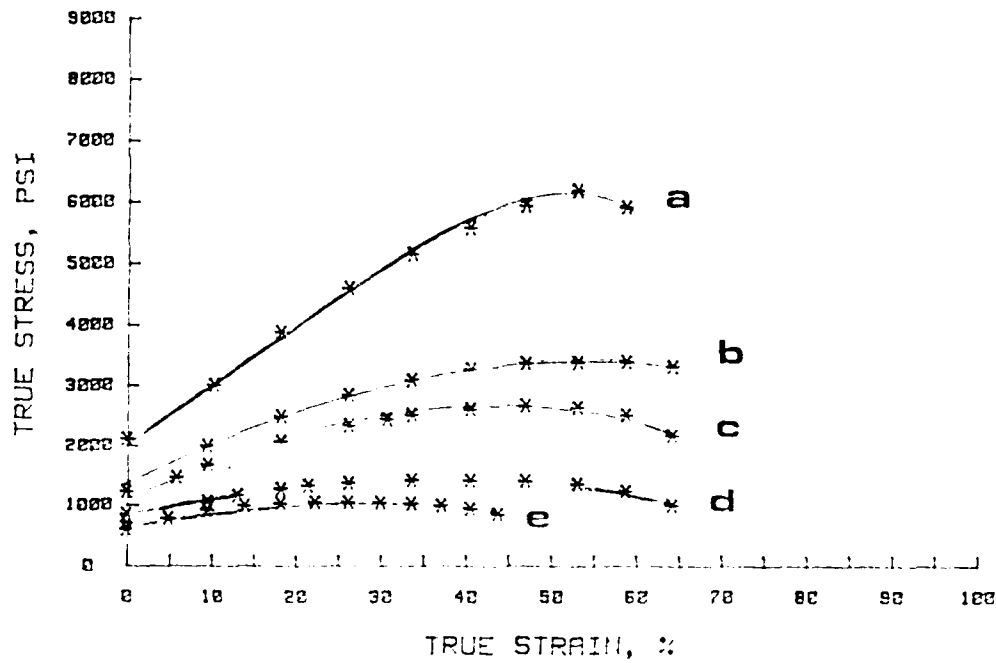
Figure 8 illustrates the effect of Li concentration. Two samples, one of 1.0 and the other of 0.5 weight percent Li, were tested at 250° C and a strain rate of  $1.67 \times 10^{-2} \text{ sec}^{-1}$ . The 1.0 percent Li alloy exhibits a high yield strength and a much higher rate of subsequent strain hardening. The ductility of the two materials is the same, reflecting the role of strain hardening in resistance to necking. At higher temperatures the strength differential remained, although to a lesser degree.



Samples of 1.0% and 0.5% Li tested at  
 250° C and  $\dot{\epsilon} = 1.67 \times 10^{-2} \text{ sec}^{-1}$ .

Figure 8. Effect of Lithium Concentration (Instron)

Figure 9 graphically illustrates the effect of temperature. Shown are test results for the 0.5 percent Li alloy tested at a strain rate of  $1.67 \times 10^{-2} \text{ sec}^{-1}$  and temperatures from 250° to 500° C. The data clearly indicates a softening of the material. At higher temperatures, deformation appears to occur at a nearly constant stress for strains above 20 percent.



Samples of 0.5% Li tested at  
 $\dot{\epsilon} = 1.67 \times 10^{-2} \text{ sec}^{-1}$  and temperatures of  
 a) 250° C      b) 350° C      c) 400° C  
 d) 450° C      e) 500° C

Figure 9. Effect of Temperature (Instron)

Creep test results, due to the variation in the selection of applied loads, do not lend themselves as readily to a comparison. However, an examination of some typical results leads to the following observations. The alloys exhibit a creep curve similar to that of pure metals. All creep curves showed a primary stage of creep followed by a constant creep rate in the secondary region and a tertiary stage of rapid elongation, necking, and failure.

The effect of the applied load can be seen by comparing Figure 10 for the 0.5 percent Li alloy tested at 400° C and 6.61 MPA to Figure 11, the 0.5 percent Li alloy tested at 400° C and 4.13 MPA. Note that the creep results are represented on various time axes. For a greater applied load, the alloy sustains a greater creep rate. Figure 12 shows similar results for the 1.0 percent Li alloy tested at 500° C and 7.5 MPA. Generally, creep rates increased as temperature increased and increased as Lithium concentration decreased.

### **C. STRAIN RATE DEPENDENCE OF STRESS**

The data of Tables 1 and 2 summarize the results of the mechanical testing and may be utilized to determine the stress and temperature dependence of the strain rate and thus facilitate determination of the underlying mechanisms of deformation. Equations 1 and 2 reduce to the form of a power-law function

$$\dot{\epsilon} = K\sigma^n$$

where  $\dot{\epsilon}$  is the strain rate,  $K$  is a temperature and structure-dependent constant,  $\sigma$  is the stress, and  $n$  is the stress exponent. Values of  $n$  for pure metals, Aluminum included, are typically equal to five.

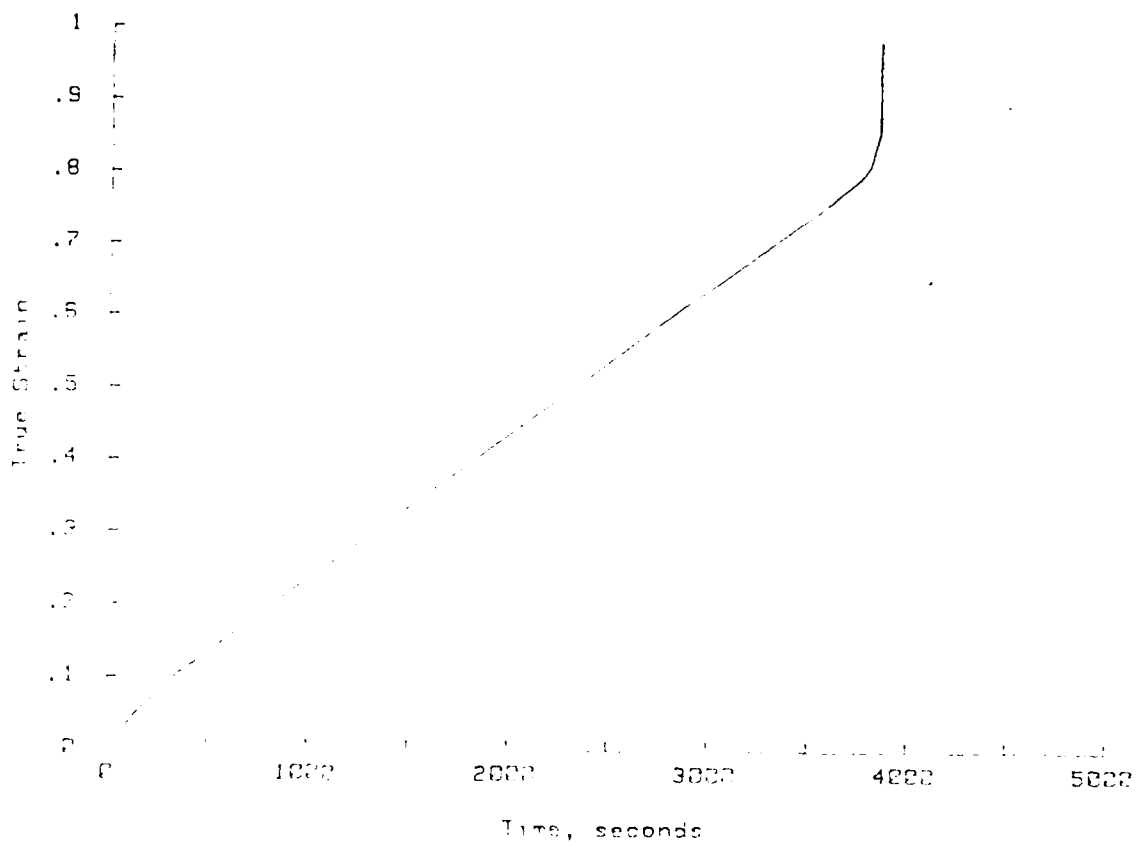


Figure 10. Creep Results for 0.5% Li at 400° C  
 $\sigma = 6.61 \text{ MPA}$ ,  $\dot{\epsilon} = 1.74 \times 10^{-4} \text{ sec}^{-1}$



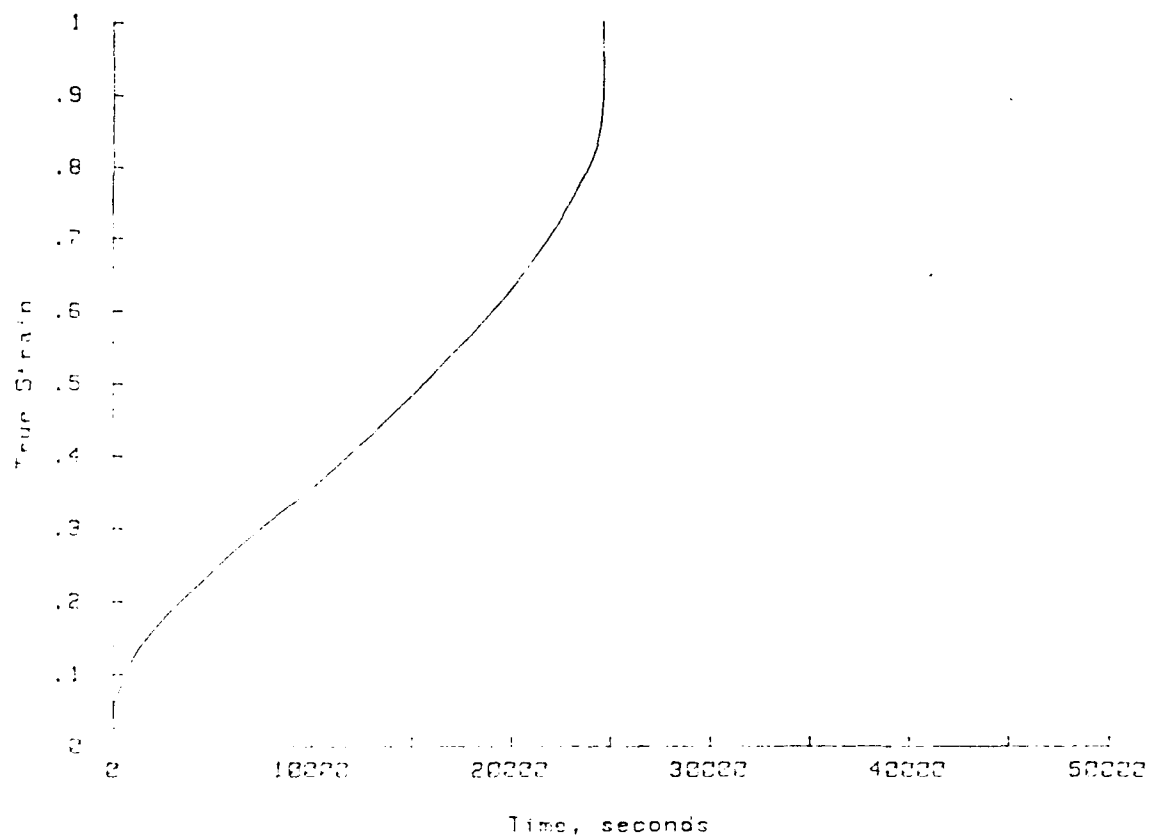


Figure 11. Creep Results for 0.5% Li at 400° C  
 $\sigma = 4.13 \text{ MPA}$ ,  $\dot{\epsilon} = 2.58 \times 10^{-5} \text{ sec}^{-1}$

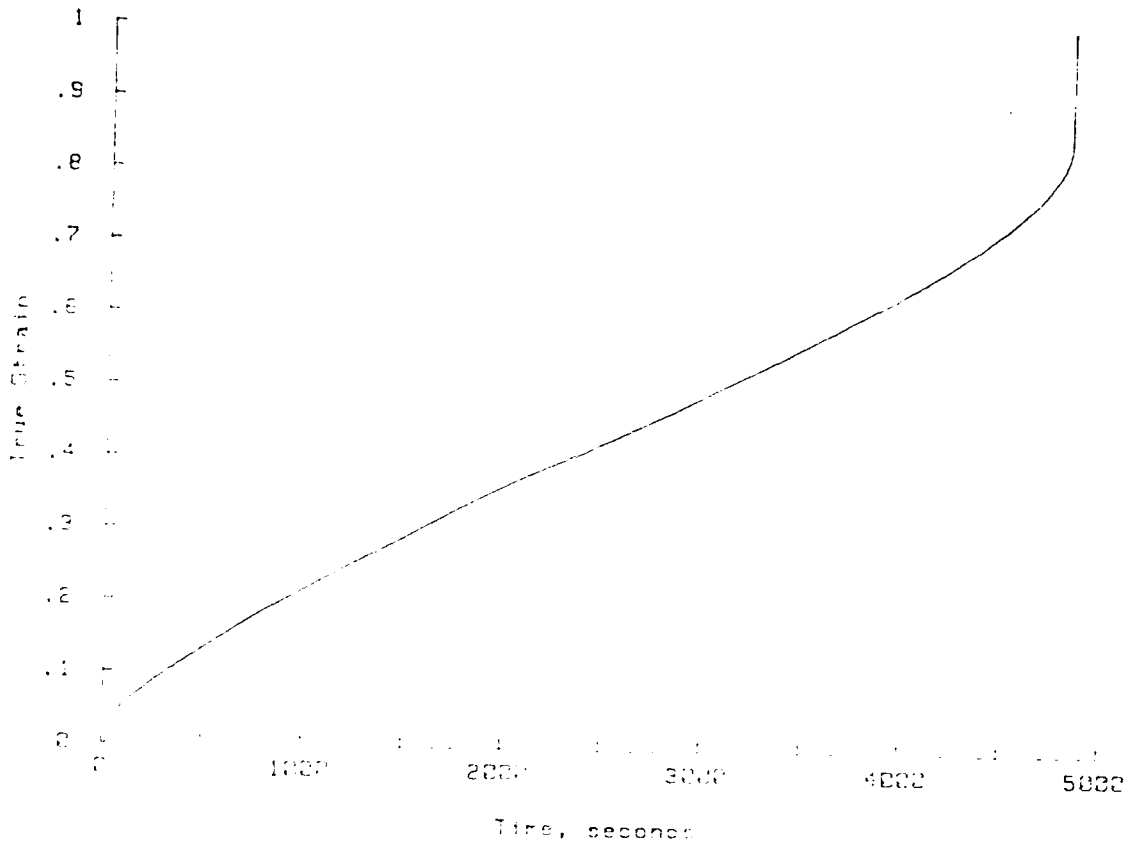


Figure 12. Creep Results for 1.0% Li at 500° C  
 $\sigma = 2.5 \text{ MPA}$ ,  $\dot{\epsilon} = 1.29 \times 10^{-4} \text{ sec}^{-1}$

TABLE 1  
SUMMARY OF 0.5% Al-Li RESULTS

Type	#	Temp (°C)	$\dot{\epsilon}$ (sec <sup>-1</sup> )	s(MPA)	log $\dot{\epsilon}$	log s	$\frac{\dot{\epsilon}}{D}$ (m <sup>-2</sup> )	$\frac{\sigma}{E}$
Instron	9	250	1.67 x 10 <sup>-2</sup>	42.54	-1.78	1.63	1.77 x 10 <sup>16</sup>	6.83 x 10 <sup>-4</sup>
Instron	10	250	1.67 x 10 <sup>-3</sup>	31.96	-2.78	1.51	1.77 x 10 <sup>15</sup>	5.13 x 10 <sup>-4</sup>
Instron	20	250	1.67 x 10 <sup>-4</sup>	18.37	-3.78	1.26	1.77 x 10 <sup>14</sup>	2.95 x 10 <sup>-4</sup>
Instron	11	300	1.67 x 10 <sup>-2</sup>	24.0	-1.78	1.38	1.01 x 10 <sup>15</sup>	3.98 x 10 <sup>-4</sup>
Instron	25	300	1.67 x 10 <sup>-3</sup>	23.37	-2.78	1.37	1.01 x 10 <sup>14</sup>	3.98 x 10 <sup>-4</sup>
Instron	33	300	1.67 x 10 <sup>-4</sup>	13.42	-3.78	1.13	1.01 x 10 <sup>13</sup>	2.226 x 10 <sup>-4</sup>
Creep	8	300	9.23 x 10 <sup>-6</sup>	12.41	-5.04	1.09	5.59 x 10 <sup>11</sup>	2.06 x 10 <sup>-4</sup>
Creep	1	300	1.42 x 10 <sup>-6</sup>	8.32	-5.85	.920	8.75 x 10 <sup>10</sup>	1.38 x 10 <sup>-4</sup>
Creep	19	300	4.71 x 10 <sup>-7</sup>	6.03	-6.33	.780	2.85 x 10 <sup>10</sup>	1.0 x 10 <sup>-4</sup>
Instron	14	350	1.67 x 10 <sup>-2</sup>	23.31	-1.78	1.37	9.12 x 10 <sup>13</sup>	4.06 x 10 <sup>-4</sup>
Instron	15	350	1.67 x 10 <sup>-3</sup>	16.42	-2.78	1.22	9.12 x 10 <sup>12</sup>	2.86 x 10 <sup>-4</sup>
Instron	22	350	1.67 x 10 <sup>-4</sup>	8.12	-3.78	.910	9.12 x 10 <sup>11</sup>	1.42 x 10 <sup>-4</sup>

TABLE I (Continued)

Type	#	Temp (°C)	$\dot{\epsilon}$ (sec <sup>-1</sup> )	s(MPA)	log $\dot{\epsilon}$	log s	$\frac{\dot{\epsilon}}{D}$ (m <sup>-2</sup> )	$\frac{\sigma}{E}$
Creep	24	350	1.49 x 10 <sup>-5</sup>	5.16	-4.83	.713	8.12 x 10 <sup>10</sup>	9 x 10 <sup>-5</sup>
Creep	13	350	2.0 x 10 <sup>-7</sup>	3.16	-6.70	.499	1.09 x 10 <sup>9</sup>	5.5 x 10 <sup>-5</sup>
Instron	18	400	1.67 x 10 <sup>-2</sup>	18.51	-1.78	1.26	1.18 x 10 <sup>13</sup>	3.33 x 10 <sup>-4</sup>
Instron	40	400	1.67 x 10 <sup>-3</sup>	7.86	-2.78	.895	1.18 x 10 <sup>12</sup>	1.43 x 10 <sup>04</sup>
Creep	7	400	1.74 x 10 <sup>-4</sup>	6.61	-3.76	.820	1.23 x 10 <sup>11</sup>	1.20 x 10 <sup>-4</sup>
Creep	3	400	2.58 x 10 <sup>-5</sup>	4.13	-4.59	.616	1.82 x 10 <sup>10</sup>	7.52 x 10 <sup>-5</sup>
Instron	12	450	1.67 x 10 <sup>-2</sup>	9.72	-1.78	.988	2.02 x 10 <sup>12</sup>	1.87 x 10 <sup>-4</sup>
Instron	31	450	1.67 x 10 <sup>-3</sup>	5.81	-2.78	.764	2.02 x 10 <sup>11</sup>	1.06 x 10 <sup>-4</sup>
Instron	36	450	1.67 x 10 <sup>-4</sup>	3.46	-3.78	.539	2.02 x 10 <sup>10</sup>	6.66 x 10 <sup>-5</sup>
Instron	28	500	1.67 x 10 <sup>-2</sup>	7.16	-1.78	.855	4.34 x 10 <sup>11</sup>	1.43 x 10 <sup>-4</sup>
Instron	35	500	1.67 x 10 <sup>-3</sup>	4.17	-2.78	.620	4.34 x 10 <sup>10</sup>	8.33 x 10 <sup>-5</sup>
Instron	34	500	1.67 x 10 <sup>-4</sup>	1.77	-3.78	.248	4.34 x 10 <sup>9</sup>	4.54 x 10 <sup>-5</sup>
Creep	27	500	5.5 x 10 <sup>-6</sup>	1.21	-5.26	.083	1.43 x 10 <sup>8</sup>	2.42 x 10 <sup>-5</sup>
Creep	4	500	1.80 x 10 <sup>-6</sup>	1.06	-5.42	.028	4.75 x 10 <sup>7</sup>	2.13 x 10 <sup>-5</sup>

TABLE 2  
SUMMARY OF 1.0% Al-Li RESULTS

Type	#	Temp (°C)	$\dot{\epsilon}$ (sec <sup>-1</sup> )	s(MPA)	log $\dot{\epsilon}$	log s	$\frac{\dot{\epsilon}}{D}$ (m <sup>-2</sup> )	$\frac{\sigma}{E}$
Instron	48	250	1.67 x 10 <sup>-2</sup>	61.36	-1.78	1.79	1.77 x 10 <sup>16</sup>	9.85 x 10 <sup>-4</sup>
Instron	79	250	1.67 x 10 <sup>-3</sup>	48.12	-2.78	1.68	1.77 x 10 <sup>15</sup>	7.73 x 10 <sup>-4</sup>
Instron	71	250	1.67 x 10 <sup>-4</sup>	20.93	-3.78	1.32	1.77 x 10 <sup>14</sup>	3.36 x 10 <sup>-4</sup>
Creep	44	250	6.68 x 10 <sup>-6</sup>	19.95	-5.18	1.30	7.09 x 10 <sup>12</sup>	3.2 x 10 <sup>-4</sup>
Instron	76	300	1.67 x 10 <sup>-2</sup>	41.33	-1.78	1.62	1.01 x 10 <sup>15</sup>	6.85 x 10 <sup>-4</sup>
Instron	58	300	1.67 x 10 <sup>-3</sup>	20.11	-2.78	1.30	1.01 x 10 <sup>14</sup>	3.34 x 10 <sup>-4</sup>
Instron	52	300	1.67 x 10 <sup>-4</sup>	15.37	-3.78	1.19	1.01 x 10 <sup>13</sup>	2.55 x 10 <sup>-4</sup>
Creep	51	300	4.65 x 10 <sup>-6</sup>	9.05	-5.04	1.09	2.81 x 10 <sup>11</sup>	1.5 x 10 <sup>-4</sup>
Creep	43	300	2.90 x 10 <sup>-8</sup>	4.22	-5.85	.920	1.77 x 10 <sup>9</sup>	7.0 x 10 <sup>-5</sup>
Instron	61	350	1.67 x 10 <sup>-2</sup>	23.35	-1.78	1.37	9.12 x 10 <sup>13</sup>	4.07 x 10 <sup>-4</sup>
Instron	66	350	1.67 x 10 <sup>-3</sup>	19.75	-2.78	1.30	9.12 x 10 <sup>12</sup>	3.44 x 10 <sup>-4</sup>
Instron	42	350	1.67 x 10 <sup>-4</sup>	8.63	-3.78	.936	9.12 x 10 <sup>11</sup>	1.5 x 10 <sup>-4</sup>

TABLE 2 (Continued)

Type	#	Temp (°C)	$\dot{\epsilon}$ (sec <sup>-1</sup> )	s(MPA)	log $\dot{\epsilon}$	log s	$\frac{\dot{\epsilon}}{D}$ (m <sup>-2</sup> )	$\frac{\sigma}{E}$
Creep	70	350	8.82 x 10 <sup>-6</sup>	6.31	-5.05	.799	4.82 x 10 <sup>10</sup>	1.10 x 10 <sup>-4</sup>
Instron	73	400	1.67 x 10 <sup>-2</sup>	14.47	-1.78	1.16	1.18 x 10 <sup>13</sup>	2.63 x 10 <sup>-4</sup>
Instron	59	400	1.67 x 10 <sup>-3</sup>	10.43	-2.78	1.02	1.18 x 10 <sup>12</sup>	1.9 x 10 <sup>-4</sup>
Creep	46	400	3.8 x 10 <sup>-4</sup>	7.14	-3.42	.85	2.68 x 10 <sup>11</sup>	1.3 x 10 <sup>-4</sup>
Creep	54	400	7.66 x 10 <sup>-6</sup>	3.84	-5.12	.58	5.40 x 10 <sup>9</sup>	7 x 10 <sup>-5</sup>
Instron	49	450	1.67 x 10 <sup>-2</sup>	10.64	-1.78	1.03	2.02 x 10 <sup>12</sup>	2.05 x 10 <sup>-4</sup>
Instron	69	450	1.67 x 10 <sup>-3</sup>	6.26	-2.78	.79	2.02 x 10 <sup>11</sup>	1.21 x 10 <sup>-4</sup>
Creep	64	450	2.18 x 10 <sup>-4</sup>	3.64	-3.66	.56	2.34 x 10 <sup>10</sup>	7 x 10 <sup>-5</sup>
Creep	60	450	1.28 x 10 <sup>-5</sup>	2.08	-4.89	.32	1.55 x 10 <sup>9</sup>	4 x 10 <sup>-5</sup>
Instron	68	500	1.67 x 10 <sup>-2</sup>	7.33	-1.78	.865	4.34 x 10 <sup>11</sup>	1.47 x 10 <sup>-4</sup>
Instron	55	500	1.67 x 10 <sup>-3</sup>	4.62	-2.78	.670	4.34 x 10 <sup>10</sup>	9.24 x 10 <sup>-5</sup>
Creep	77	500	1.29 x 10 <sup>-4</sup>	2.50	-4.29	.398	3.34 x 10 <sup>9</sup>	5 x 10 <sup>-5</sup>
Creep	41	500	3.03 x 10 <sup>-5</sup>	1.50	-4.52	.176	7.86 x 10 <sup>8</sup>	3 x 10 <sup>-5</sup>
Creep	53	500	5.17 x 10 <sup>-6</sup>	1.25	-5.29	.097	1.34 x 10 <sup>8</sup>	2.5 x 10 <sup>-5</sup>

The experimental values of  $\dot{\epsilon}$  were plotted versus  $\sigma$  on double logarithmic axes for each test temperature (Figures 13 and 14). A straight line was fitted to all points for each test temperature. Considerable scatter is evident in the data for some temperatures. However, for both alloys the stress exponent  $n$  appears to be 5 to 7 at temperatures of 250° C and 300° C, and to decrease to values of 4.5 to 5.0 at temperatures above 300° C. These  $n$  values, calculated from the data by means of a linear regression, are compiled in Table 3. From these  $n$  values, it is surmised that the mechanism of creep in these alloys is similar to that of pure Aluminum, which deforms by the glide and climb of dislocations, with diffusion-controlled climb determining the overall rate of straining.

TABLE 3  
CALCULATED VALUES OF  $n$

Experimental Values of  $n$  Determined by Linear Regression

T (°C)	Value of $n$	
	0.5% Li	1.0% Li
250	5.2	5.4
300	7.1	6.1
350	5.2	4.9
400	4.4	5.6
450	4.5	4.3
500	4.3	4.3

#### D. EFFECT OF DEFORMATION ON MICROSTRUCTURE

Optical microscopy studies were conducted upon samples representing both alloy compositions. These samples were obtained from the deformed gage section after straining to failure at a rate of 1.67 x

10<sup>-2</sup> S<sup>-1</sup> in the Instron at temperatures of 300°, 400°, and 500° C. Figure 15 shows the 0.5 percent Li alloy at 400° C. The grains show a moderate elongation along the deformation axis, with a slight serration of the grain boundaries. At 500° C (Figure 16), the elongation is also noted and the boundary serrations have become very pronounced.

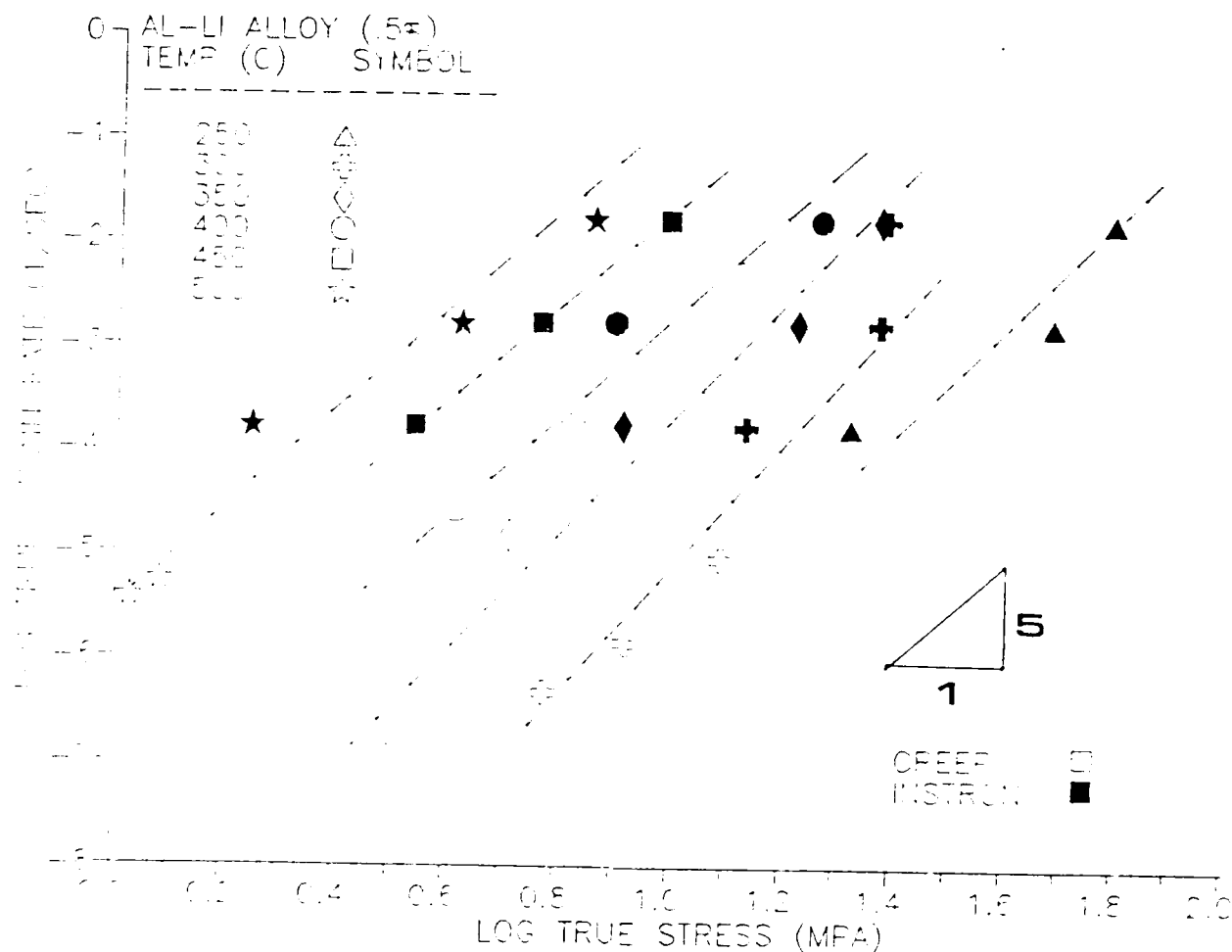


Figure 13. Log  $\dot{\epsilon}$  vs. Log  $\sigma$  Results (0.5% Li)



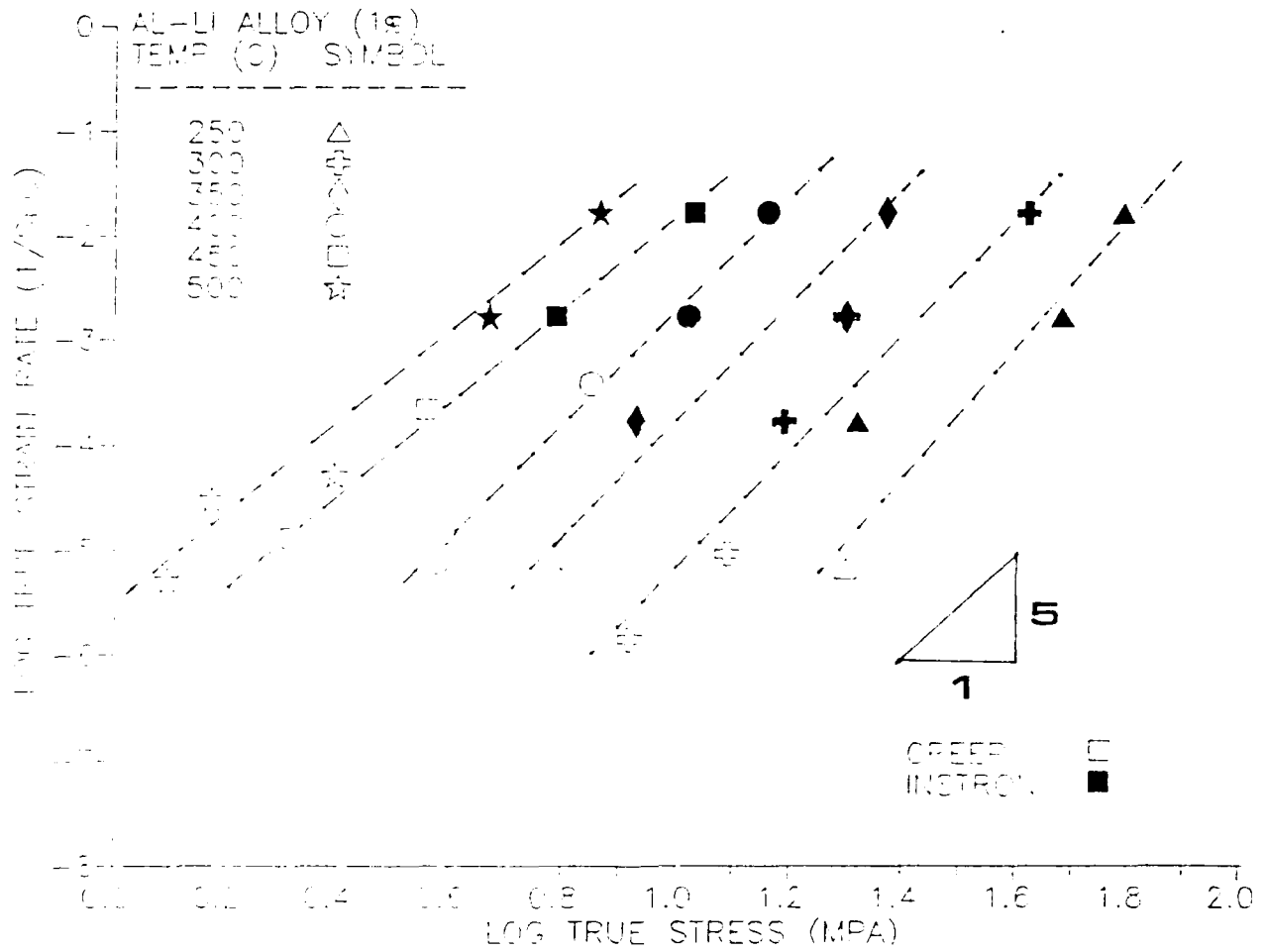


Figure 14. Log  $\dot{\epsilon}$  vs. Log  $\sigma$  Results (1.0% Li)

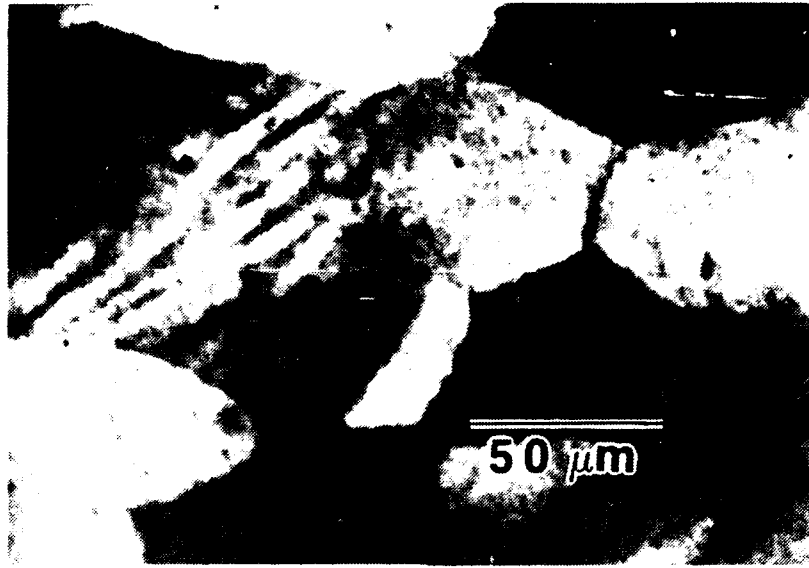


Figure 15. 0.5% Li at 400° C,  $\dot{\epsilon} = 1.67 \times 10^{-2} \text{ sec}^{-1}$

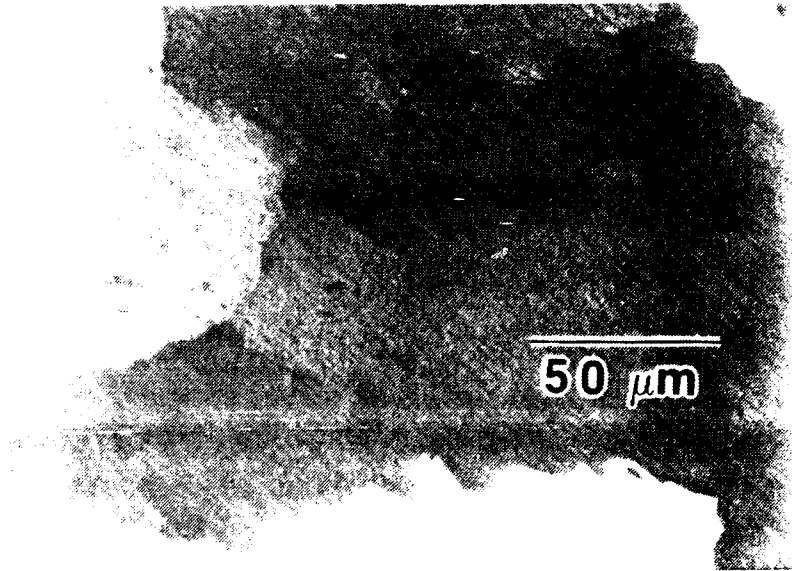


Figure 16. 0.5% Li at 500° C,  $\dot{\epsilon} = 1.67 \times 10^{-2} \text{ sec}^{-1}$

In the 1.0 percent Li alloy, deformed at 400° C (see Figure 17), grains are more elongated than those seen in the 0.5 percent Li

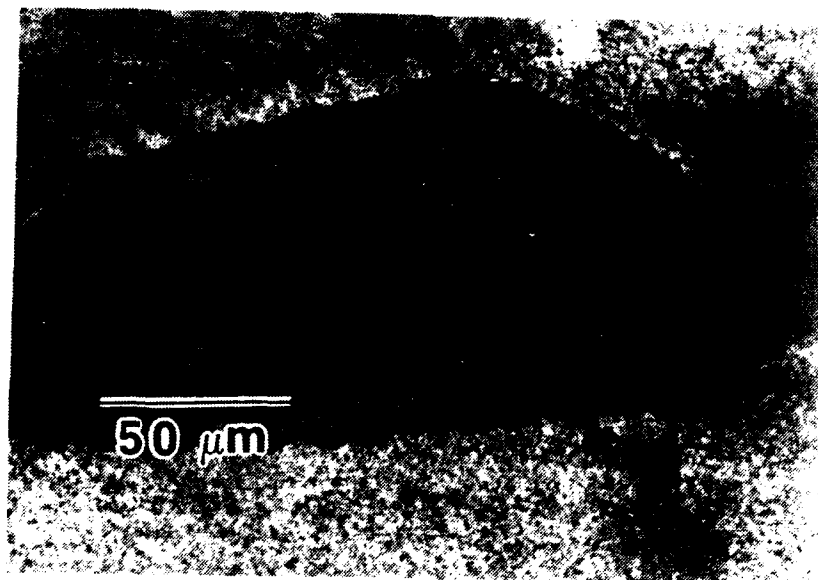


Figure 17. 1.0% Li at 400° C,  $\dot{\epsilon} = 1.67 \times 10^{-2} \text{ sec}^{-1}$

counterpart and the grain boundary serration exists to a greater degree. The 500° C sample (Figure 18) also exhibits an extreme degree of serration but with a finer grain size apparent than observed in the sample tested at 400° C. Micrographs of the 300° C sample exhibited moderate grain elongation but no visible irregularities of the grain boundaries.

The observed grain boundary serration is characteristic of subgrain formation and is also consistent with the deformation characteristics of pure Aluminum in that climb control of deformation is accompanied by subgrain formation.

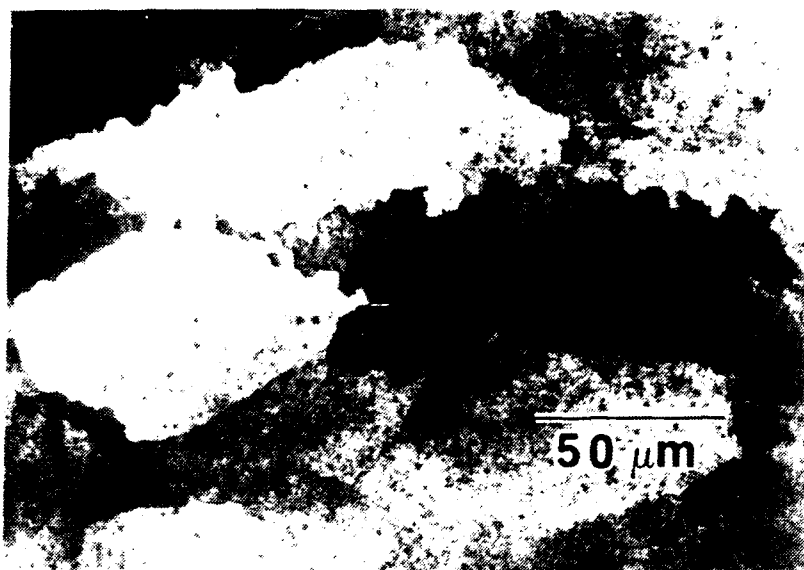


Figure 18. 1.0% Li at 500° C,  $\dot{\epsilon} = 1.67 \times 10^{-2} \text{ sec}^{-1}$

#### E. ACTIVATION ENERGY

Assuming that the strain rate follows an Arrhenius temperature dependence at constant stress, a value for the activation energy of deformation can be obtained:

$$Q_c = -2.303R \frac{\Delta \log_{10} \dot{\epsilon}}{\Delta(\frac{1}{T})} \quad (4)$$

where T is in degrees Kelvin and R = 1.98 cal/mole K.

Using the straight lines plotted in Figures 13 and 14 as the relationship between log (strain rate) and log (stress), activation energy values may be obtained. This is accomplished by obtaining values of log  $\dot{\epsilon}$  and  $\frac{1}{T}$  at constant stress and the activation energy values obtained are summarized in Table 4. Although the results again exhibit some data scatter, the values of  $Q_c$  in the 0.5 percent Li alloy at tempera-

tures below 300° C and above 450° C for the 1.0 percent Li alloy are appreciably lower than the remainder of values. It can also be seen that for temperatures between 300° and 450° C, the activation energy of deformation for the alloys is between 40 and 50 K cal/mole. In contrast, experimental values of  $Q_C$  for pure Aluminum over the same temperature interval are 35 Kcal/mole [Ref. 11]. Therefore, although the Al-Li alloy exhibits a similar stress dependence and the formation of subgrain structures as pure Aluminum, the values of activation energy for deformation are appreciably greater.

TABLE 4  
SUMMARY OF ACTIVATION ENERGIES

Activation Energy at Constant Stress

Temperature Interval (°C)	Log of Applied Stress	Activation Energy (Kcal/mole)	Lithium Concentration	
250-300	1.4	30.6	0.5%	
300-350	1.3	26		
	1.0	36.4		
	.7	46.2		
350-400	1.0	38.3		
	.6	45.9		
400-450	.6	48.8		
450-500	.6	50.7		
250-300	1.7	31.6		1.0%
	1.3	45.6		
300-350	1.46	40.4		
	.84	39.7		
350-400	1.3	41.0		
	.7	44.8		
400-450	1.0	38.1		
	.6	53.8		
450-500	.8	31.3		

The activation energy for creep can be considered a summation of self-diffusion, stacking fault energy, and modulus components (see equations 5 and 6). As noted earlier in Chapter II, the addition of Lithium to Aluminum has the effect of increasing the modulus due to its effect on bonding. Also, ordering in the structure of the solid solution is seen. This may result in a temperature-dependent modulus, in conjunction with any temperature effects on stacking fault energy, and could account for the values of  $Q_C$  being greater than those for self-diffusion.

#### **F. EFFECT OF LITHIUM CONCENTRATION ON STRENGTH**

An important goal of this research was to determine the effect of the Li addition on the elevated temperature creep strength of aluminum. Test results from both 0.5 percent Li and 1.0 percent Li as well as data obtained by Ellison [Ref. 7] for 2.0 percent Li were compared for each of three test temperatures: 250°, 350°, and 500° C (Figures 19, 20, 21). For comparison purposes, data from the literature [Ref. 11] for pure Aluminum at the appropriate temperature was plotted as a dashed line. It can be readily discerned that as the concentration of Lithium increases, the necessary applied stress to attain a given strain rate increases, implying a stronger material under creep. Data scatter from the 0.5 percent Li and the 1.0 percent Li alloys tends to blur the differences with pure Aluminum. This scatter could indicate a necessity for a refinement of testing procedures or could indicate the presence of other factors not considered which have a greater effect at lower temperatures. The strengthening

implied by the lower Li content alloys is confirmed by the 2.0 weight percent Li alloy results.

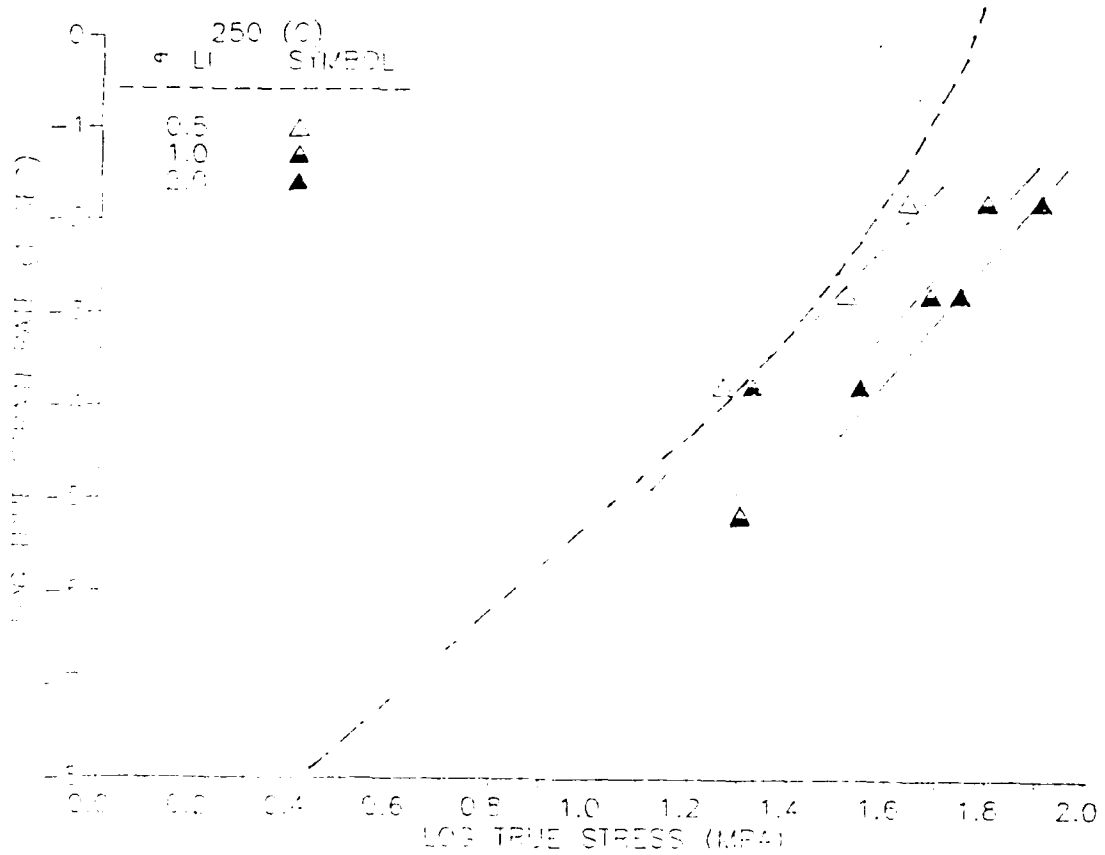


Figure 19.  $\epsilon$  vs.  $\sigma$  at 250° C

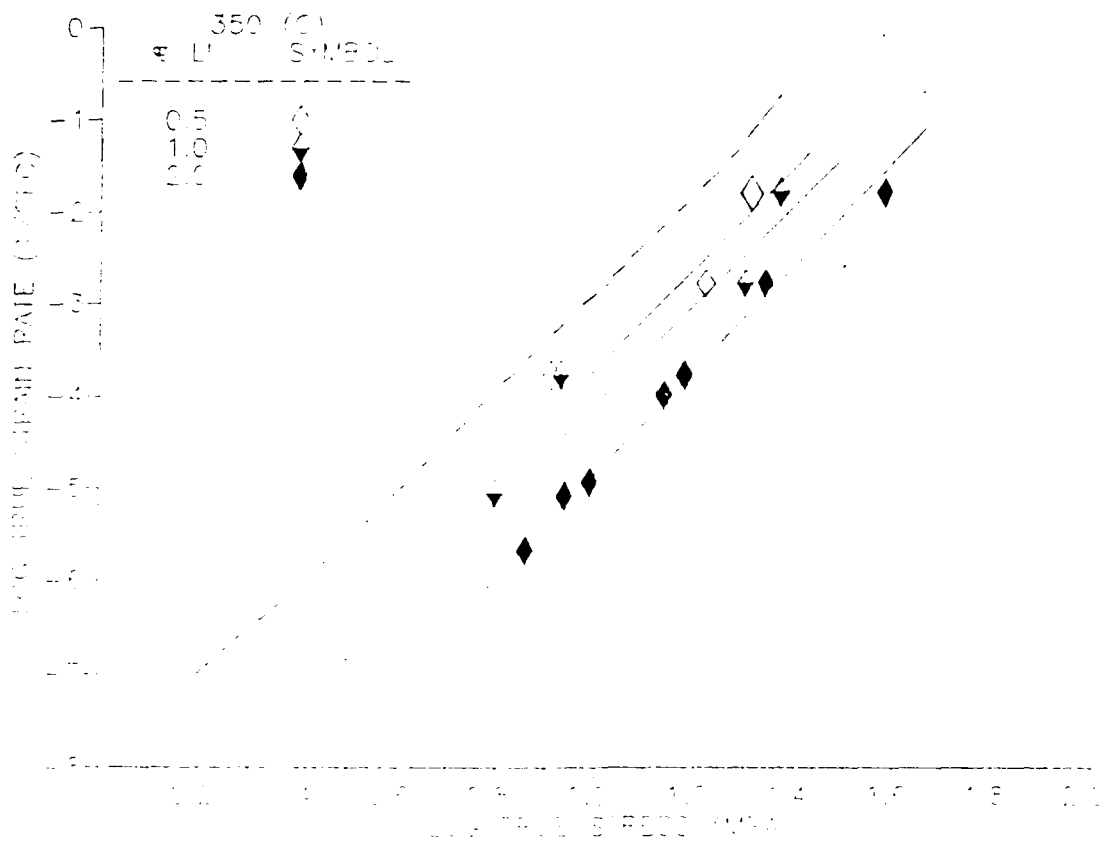


Figure 20.  $\dot{\epsilon}$  vs.  $\sigma$  at 350° C



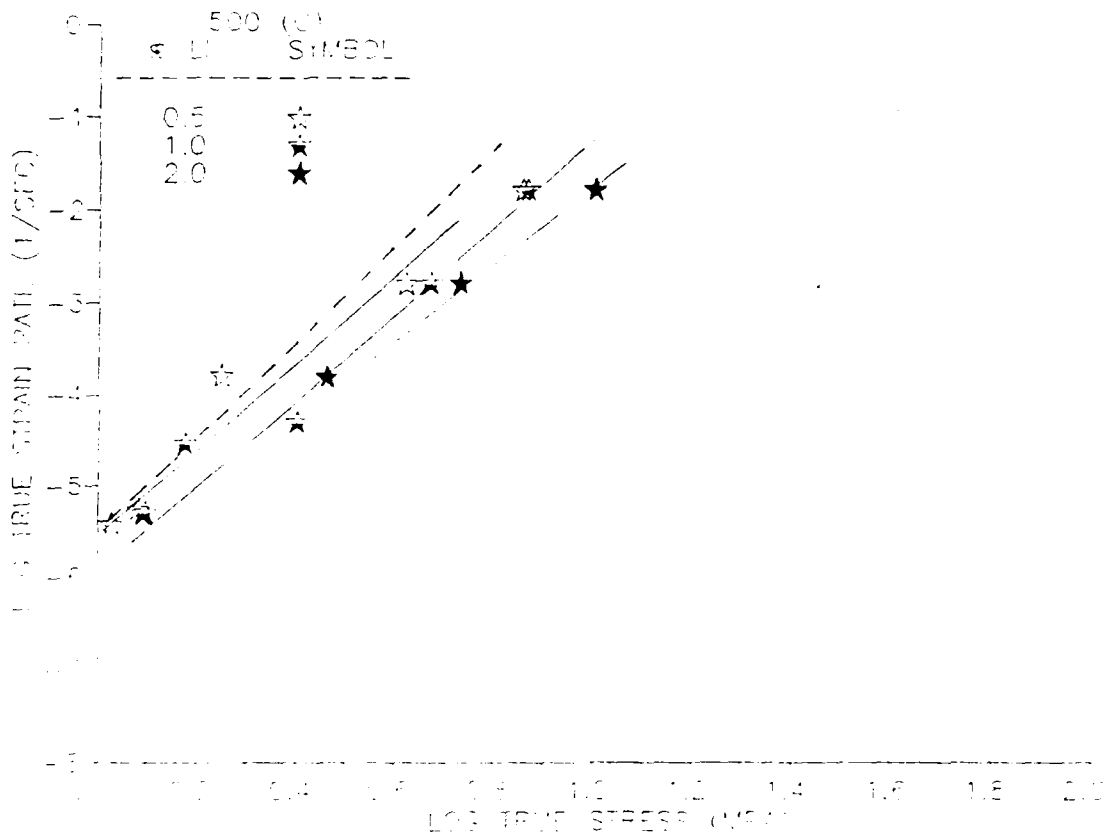


Figure 21.  $\dot{\epsilon}$  vs.  $\sigma$  at 500° C

Furukawa [Ref. 12] attributes the strengthening of Aluminum by Lithium at lower temperatures to the formation of coherent  $\delta'$  ( $\text{Al}_3\text{Li}$ ) precipitates which are homogeneously distributed throughout the Aluminum matrix. To date, however, no evidence of this metastable precipitate has been found in Lithium concentrations less than 1.6 weight percent. In his work, Ellison [Ref. 7] has provided evidence that the Al-Li solid solution may be an ordered solution, at least with 2 weight percent Li present. The presence of superlattice reflections

was cited as evidence for this in the absence of any precipitates. This is consistent with reports by Radmilovic, Fox, and Thomas [Ref. 5], who also report evidence for ordering in the solid solution at temperatures above the solvus for Li in the alloy. These data suggest that such ordering may extend to Li content as low as 0.5 percent and contribute to the creep strength of these alloys.

### **G. NORMALIZED RESULTS**

Further insight can be obtained by replotting these data as diffusion-compensated strain rate versus modulus-compensated stress. Diffusion and modulus data were those for pure Aluminum because data for the alloys is unavailable. These results are represented on log/log scales (Figures 22, 23) and compared to similar data obtained from the literature [Ref. 5] for pure Aluminum (dashed line). Here the data scatter is somewhat less apparent and the data appears similar to the Aluminum data, with the same stress dependence, but is uniformly stronger with the Lithium addition. Upon closer examination, however, it can be seen that as temperature decreases, the degree of alloy strengthening relative to the pure Aluminum increases. This may indicate that the temperature dependence of the normalizing values for the alloy is different from the temperature dependence for those of the pure metal. Stacking fault energy and modulus are a function of temperature. If these functions for the alloy are the same as the pure metal, then one could expect little or no variation in the normalized data for the two cases. However, as noted earlier, the activation energy for the alloys is appreciably greater than for the pure metal. This may

be an indication that the temperature dependence of stacking fault energy and modulus is also different for the alloy, leading to the aforementioned scatter of data in the normalized presentation.

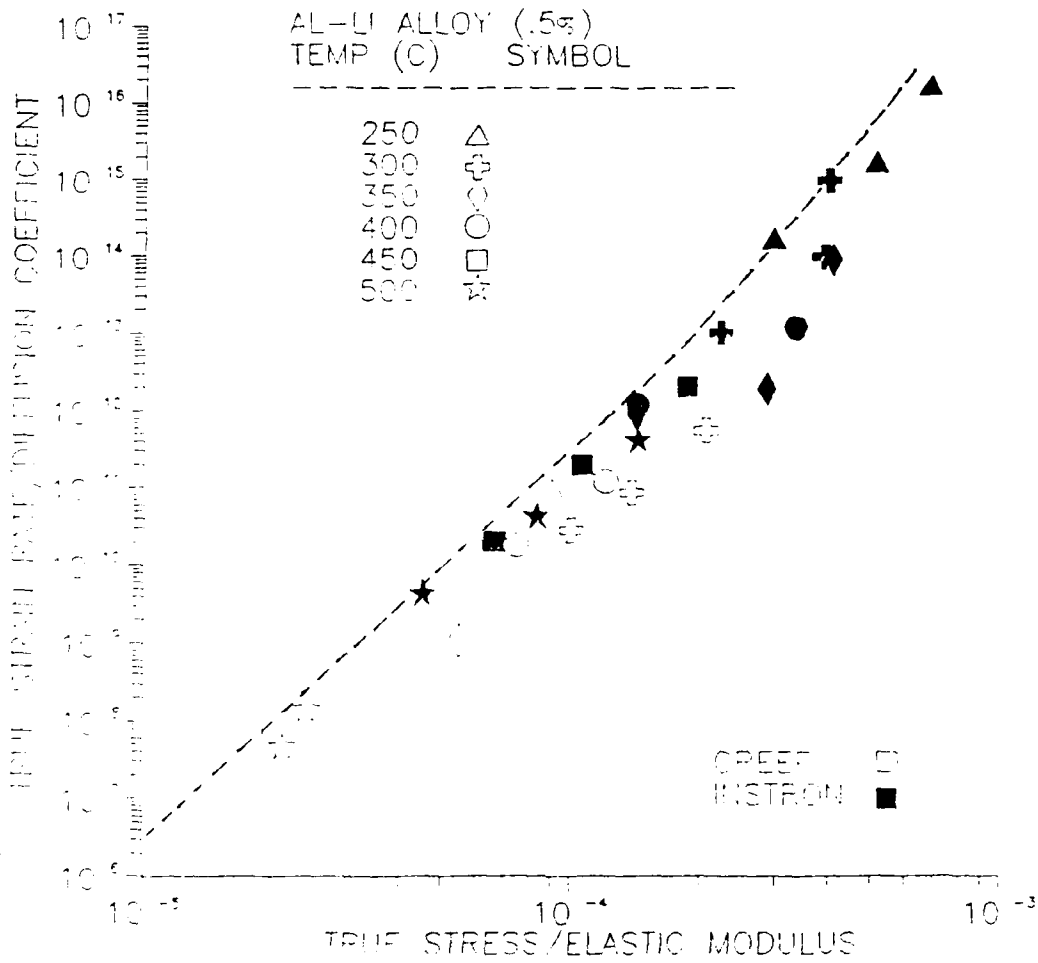


Figure 22. Normalized Results 0.5% Li

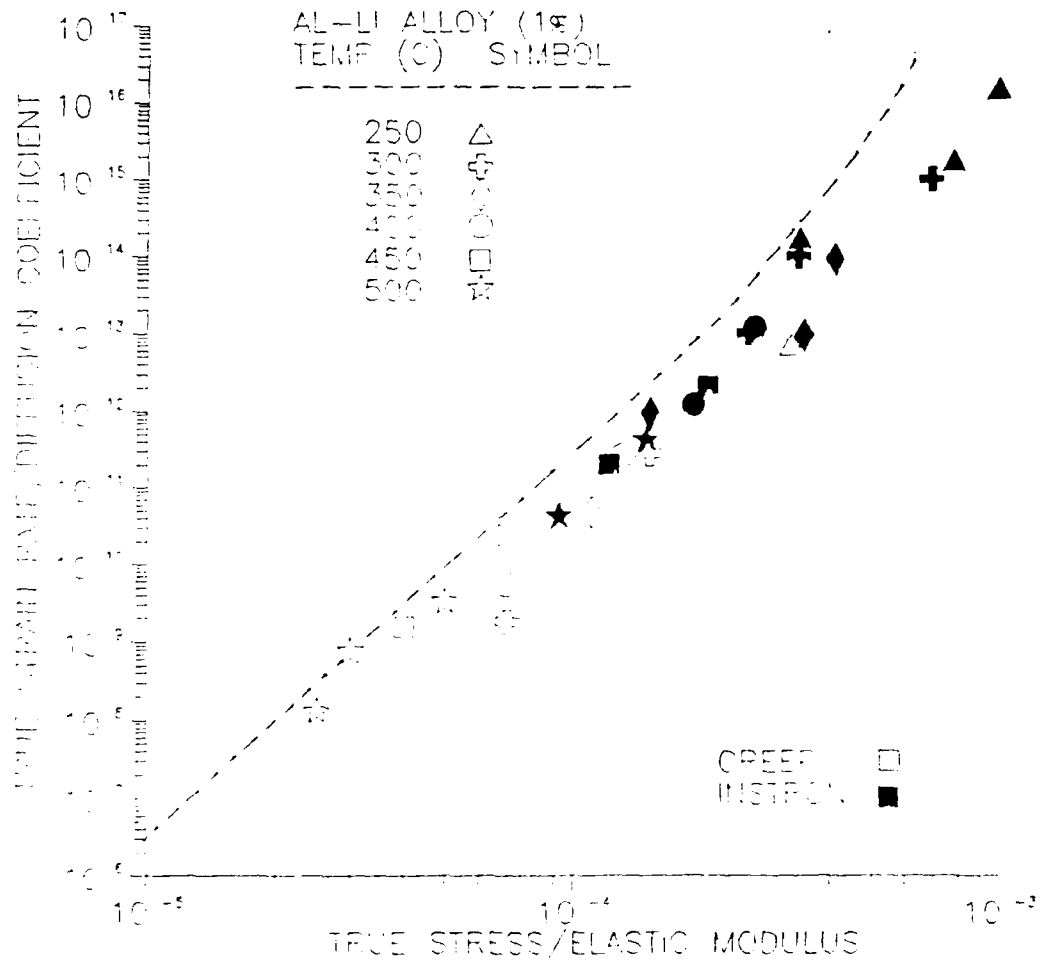


Figure 23. Normalized Results 1.0% Li

## V. CONCLUSIONS

The following conclusions can be drawn concerning the behavior and characteristics of binary Aluminum-Lithium alloys of less than 2.0 percent Lithium:

1. The alloys exhibit a creep response consisting of a primary, secondary, and tertiary phase.
2. The alloys exhibit the same stress dependence as pure Aluminum.
3. The controlling mechanism of creep is that of dislocation climb as evidenced by the formation of subgrains.
4. Lithium addition increases the activation energy for creep to a greater value than that of diffusion for pure Aluminum. This is possibly accomplished by an alteration of the temperature dependence of modulus or stacking fault energy or through additional processes such as ordering of the Lithium in the solid solution.
5. Lithium additions modestly increase the strength of pure Aluminum at elevated temperatures.

It is recommended that testing continue with these two alloys. A larger body of data must be accumulated to eliminate the uncertainties of the stress relation (value of  $n$ ) and to reduce the effect of data scatter. Transmission electron microscopy should be used to determine

the microstructural characteristics of the alloys, as influenced by a  
lattice deformation.

## LIST OF REFERENCES

1. Divecha, A. P., and Karmarker, S. D., "The Search for Al-Li Alloys," *Advanced Materials and Processes*, v. 130, pp. 74-79, 1986.
2. Sigli, G., and Sanchez, J. M., "Calculation of Phase Equilibrium in Al-Li Alloys," *Acta Metallurgica*, v. 34, n. 6, pp. 1021-1028, 1986.
3. McAlister, A. J., "Al-Li Phase Diagram," *Binary Alloy Phase Diagrams*, ed. Massalski, T. B., p. 128, American Society for Metals, 1986.
4. Fox, A. G., "Structure Factors and Debye Temperatures of Al-Li Solid Solution Alloys," *Acta Crystallographa*, pp. 260-265, 1989.
5. Radmilovic, V., Fox, A. G., Fisher, R. M., and Thomas, G., "Lithium Depletion in Precipitate Free Zones in Al-Li Base Alloys," *Scripta Metallurgica*, v. 23, pp. 75-79, 1989.
6. Sherby, O. D., and Burke, P., "Mechanical Behavior of Crystalline Solids at Elevated Temperature," *Progress in Materials Science*, pp. 325-386, 1987.
7. Ellison, K., unpublished research, Naval Postgraduate School, Monterey, California, March 1987.
8. Matlock, D. K., Ph.D. Dissertation, Stanford University, Palo Alto, California, August 1972.
9. Garafalo, F., and Richmond, W. F., "Design of Apparatus for Constant-Stress or Constant Load Creep Tests," *Journal of Basic Engineering*, pp. 287-293, 1962.
10. Coughlan, W. A., "Constant Stress Continuous Load Compression Creep Machine for Small Single Crystals," *The Review of Scientific Instruments*, pp. 464-467, 1971.
11. Wu, Y. W., and Sherby, O. D., "Unification of Harper-Don and Power Law Creep through Consideration of Internal Stress," *Acta Metallurgica*, v. 32, pp. 1561-1572, 1984.

12. Furukawa, M., Yasuhiro, M., and Minoru, N., "Strengthening Mechanisms in Al-Li Alloys Containing Coherent Ordered Particles," *Transactions of the Japan Institute of Metals*, v. 26, no. 4, pp. 230-235, 1985.



## INITIAL DISTRIBUTION LIST

	<u>No. Copies</u>
1. Defense Technical Information Center Cameron Station Alexandria, VA 22304-6145	2
2. Library, Code 0142 Naval Postgraduate School Monterey, CA 93943-5002	2
3. Department Chairman, Code 69 Department of Mechanical Engineering Naval Postgraduate School Monterey, CA 93943-5000	1
4. Professor T. R. McNelley, Code 69Mc Department of Mechanical Engineering Naval Postgraduate School Monterey, CA 93943-5000	5
5. Dr. D. J. Michel, Code 6390 High Temperature Materials Branch Naval Research Laboratory Washington, D.C. 20375	1
6. LCDR David W. Taylor 15 High Meadows Drive Mullica Hill, NJ 08062	1